Journal of
Medicinal Chemistry

Drug Annotation

Discovery of GS-9688 (Selgantolimod), as a Potent and Selective Oral Toll-like Receptor 8 Agonist for the Treatment of Chronic Hepatitis B

Richard L. Mackman, Michael Mish, Gregory Chin, Jason Perry, Todd C. Appleby, Vangelis Aktoudianakis, Sammy Metobo, Peter Pyun, Congrong Niu, Stephane Daffis, Helen Yu, Jim Zheng, Armando Garcia Villaseñor, Jeff Zablocki, Jason Chamberlain, Haolun Jin, Gary Lee, Kimberly Suekawa-Pirrone, Rex Santos, William E. Delaney, and Simon Fletcher

J. Med. Chem., **Just Accepted Manuscript** • DOI: 10.1021/acs.jmedchem.0c00100 • Publication Date (Web): 14 May 2020

Just Accepted

is published by the American Chemical Society. 1155 Sixteenth Street N.W., Washington, DC 20036

Discovery of GS-9688 (Selgantolimod) as a Potent and Selective Oral Toll-Like Receptor 8 Agonist for the Treatment of Chronic Hepatitis B

Richard L. Mackman,[†,*] Michael Mish,[†] Gregory Chin,[†] Jason K. Perry,[†] Todd Appleby,[†] Vangelis Aktoudianakis,[†] Sammy Metobo,[†] Peter Pyun,[†] Congrong Niu,[†] Stephane Daffis,[†] Helen Yu,[†] Jim Zheng,[†] Armando G. Villasenor,[†] Jeff Zablocki,[†,‡] Jason Chamberlain,[†,∥] Haolun Jin,[†] Gary Lee,[†] Kimberley Suekawa-Pirrone,[†] Rex Santos,[†] William E. Delaney IV,[†] Simon P. Fletcher[†]

[†]Gilead Sciences, Inc., 333 Lakeside Drive, Foster City, California 94404, United States

ABSTRACT

Toll-like receptor 8 (TLR8) recognizes pathogen-derived single stranded RNA fragments to trigger innate and adaptive immune responses. Chronic hepatitis B (CHB) is associated with a dysfunctional immune response, and therefore a selective TLR8 agonist may be an effective treatment option. Structure based optimization of a dual TLR7/8 agonist led to the identification of the selective TLR8 clinical candidate (*R*)-2-((2-amino-7-fluoropyrido[3,2-*d*]pyrimidin-4-yl)amino)-2-methylhexan-1-ol (GS-9688, (*R*)-**7**). Potent TLR8 agonism (IL-12p40 EC_{50}=220 nM) and >100-fold TLR7 selectivity (IFN-α EC_{50}>50 μM) was observed in human peripheral blood mononuclear cells (PBMCs). The TLR8-ectodomain: (*R*)-**7** complex confirmed TLR8 binding and a direct ligand interaction with TLR8 residue Asp545. Oral (*R*)-**7** had good absorption and high first pass clearance in preclinical species. A reduction in viral markers was observed in HBV-infected primary human hepatocytes treated with media from PBMCs stimulated with (*R*)-**7**, supporting the clinical development of (*R*)-**7** for the treatment of CHB.

TOC GRAPHIC

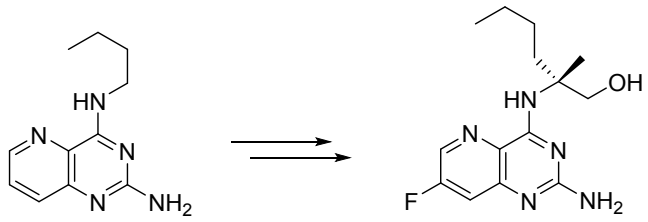

PBMC IL-12p40 EC_{50} = 1.9 μM
PBMC IFN-α EC_{50} = 2.2 μM

PBMC IL-12p40 EC_{50} = 0.22 μM
PBMC IFN-α EC_{50} >50 μM

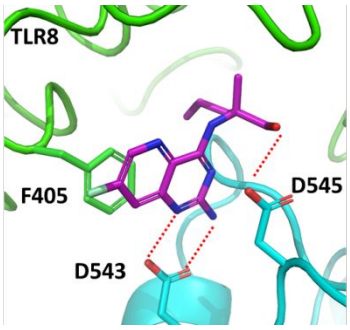

INTRODUCTION

Toll-like receptors (TLRs) are a family of membrane-bound molecular pattern recognition receptors that play a central role in the detection of molecular fragments from microorganisms. Activation of the TLRs leads to the initiation of innate and adaptive immune responses.[1] Human TLR8 is located on the endosomal membrane of a subset of immune cells, notably myeloid dendritic cells, monocytes, macrophages, and neutrophils, and recognizes single stranded RNA (ssRNA) fragments.[2] A closely related toll-like receptor, TLR7 is also located on the endosome membrane, and similarly recognizes ssRNA, but in contrast to TLR8, is predominantly expressed in plasmacytoid dendritic cells and B cells. Importantly, this orthogonal cell-specific expression pattern drives disparate immune responses upon either TLR7 or TLR8 receptor activation. TLR7 agonism predominantly induces the production of interferon-α (IFN-α), whereas TLR8 agonism stimulates the production of a variety of immunomodulatory and pro-inflammatory cytokines including interleukin-12 (IL-12), IL-18 and tumor necrosis factor-α (TNF-α).

Chronic hepatitis B (CHB) is a major global health care challenge and one of the main causes of chronic liver disease, cirrhosis and hepatocellular carcinoma. An estimated two billion people worldwide have been acutely infected with hepatitis B (HBV), of which >250 million have developed CHB, and an estimated 887,000 die annually from complications associated with CHB.[3,4] CHB is characterized by a dysfunctional or exhausted immune response and therefore it is hypothesized that TLR8 activation with a small molecule agonist could stimulate a host immune response and lead to an effective new treatment option for CHB.[5] In vitro, TLR8 small molecule agonists have been shown to stimulate a $CD8^+$ T cell response to HBsAg, a viral protein secreted from HBV-infected hepatocytes, and the TLR8-induced immunomodulatory

cytokine, IL-12, has also been shown to rescue the antiviral function of exhausted HBV-specific $CD8^+$ T cells.[6,7] IL-12 and IL-18 also strongly activate cytolytic and non-cytolytic functions of natural killer cells and mucosal-associated invariant T-cells.[8] In addition, TLR8 strongly induces TNF-α, which has been shown to drive intrahepatic $CD8^+$ T cell expansion and inhibit HBV in an adenovirus mouse model.[9] Finally, TLR8 induced cytokines including IFN-γ, IL-1β and TNF-α, have direct antiviral properties against HBV in vitro.[10-12] Taken together, these data show that TLR8 engages multiple arms of the immune system, and produces antiviral cytokines that have been shown to inhibit HBV in vitro and in vivo.

Our aim was to design an oral, selective small molecule agonist of TLR8 with good absorption and high first-pass hepatic clearance as a rational approach to induce effective pre-systemic antiviral immunity in CHB patients. Activation of TLR8 expressing immune cells in the gut following oral administration would be expected to result in the secretion of immune mediators into the portal vein that will in turn, stimulate immune cells in the liver, the organ of HBV infection. In addition, intestinal absorption of the agonist and drug exposure in the liver should lead to direct effects on intrahepatic TLR8-expressing immune cells. Provided the compound demonstrates high first pass hepatic clearance in hepatocytes, systemic exposure of the agonist would be minimized, thereby reducing undesirable side effects from systemic TLR8 agonism. TLR7 agonism with oral small molecule agents has also been hypothesized to be beneficial for CHB treatment and led to the discovery of vesatolimod from this group.[13] The design of a selective TLR8 agonist would therefore afford the flexibility to modulate both pathways independently and allow for a combination approach if applicable. This is especially important because the relative contributions of oral TLR7 and TLR8 agonism, and their disparate

immune responses to the treatment of CHB, or indeed, tolerability limitations, were largely unknown at the time.

The co-crystal X-ray structure of TLR8 ectodomain with the dual TLR7/TLR8 agonist 3M-002 (**1,** Figure 1) was recently reported and enabled a rational approach to design novel TLR8-selective agonists.[14] Compound **1** has marginal selectivity for TLR8, and is structurally-related to the TLR7 agonist imiquimod which was approved in the 1990s for the treatment of genital warts.[15,16] In contrast, Compounds **2** and **3** (VTX-2337), that contain the 2-aminoquinoline or 2-aminobenzazepine bicyclic cores have increased selectivity for TLR8 .[17,18] These scaffolds illustrate that the tricyclic core of **1** can be truncated to a quinoline or benzoazepine bicyclic heterocycle and yet retain TLR8 potency. During the course of this program additional novel TLR8 agonists were reported in the literature including the monocyclic 2,4-diaminopyrimidines **4** and **5**.[19,20]

Figure 1. TLR8 agonists

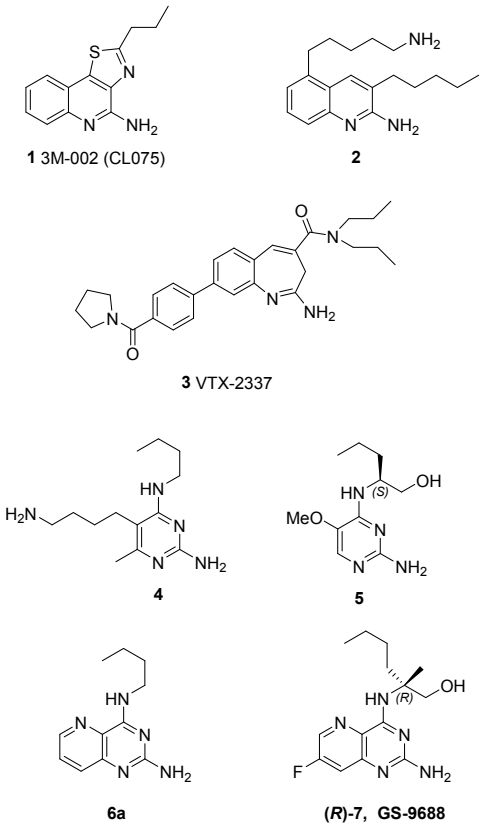

The pyrido[3,2-*d*]pyrimidine heterocycle and its preparation was familiar to this group due to its earlier inclusion in compounds that demonstrated promising anti-HCV activity.[21] Based on the same heterocycle, **6a** was identified as a moderately potent dual TLR7/8 agonist lead. Optimization of the C-4 and C-7 substituents on the heterocycle led to the identification of the TLR8 selective clinical candidate (*R*)-**7** (GS-9688, selgantolimod). The structure-activity relationships that led to the identification of (*R*)-7 as a selective TLR8 agonist are described in addition to the preclinical pharmacokinetic properties that demonstrate pre-systemic exposure and minimal oral bioavailability due to high first pass clearance. The inhibition of viral parameters in hepatitis B infected primary human hepatocytes (PHH), combined with the previously reported antiviral efficacy in the woodchuck model of CHB, support the development of (*R*)-**7** as an orally delivered, first in class, selective TLR8 agonist for the treatment of CHB.[22]

RESULTS AND DISCUSSION

A high throughput multiplex assay was developed, that quantified the levels of IL-12p40 (TLR8 cytokine) and IFN-α (TLR7 cytokine) in the supernatant of human PBMCs. Provided IL-12p40 induction was >50% of the TLR8 selective control compound **3**, a concentration for 50% maximal induction (EC_{50}) of this cytokine was calculated from the computationally fitted dose response curve. IFN-α induction values were calculated in a similar manner using the TLR7 agonist, vesatolimod, as the positive control. A single PBMC donor was used consistently during the SAR iteration to reduce assay variability. Human embryonic kidney (HEK) 293 reporter cell lines stably expressing human TLR8 or TLR7 have also been reported in the literature as a primary screening tool for the identification of TLR7 or TLR8-selective agonists.[20] However, an advantage of the robust high throughput PBMC assay developed here is that both TLR7 and TLR8 responses could be assessed in the same assay using non-transformed cells that do not overexpress the TLR receptors. Therefore a more biologically relevant functional selectivity window could be calculated based on the respective IL-12p40 and IFN-α responses in a single assay.

The active TLR8 homodimer has two equivalent agonist binding sites at the interface of the ectodomain monomers. A common feature for all the TLR8 agonists shown in Figure 1 is the presence of a weakly basic heterocyclic nitrogen, with a range of weakly basic pKa values e.g. pKa = 6.3 and 7.3 for **1** and **3** respectively. In the low pH ~4-6 environment of the endosomal compartment where TLR8 is functional, this weakly basic group is protonated. The co-crystal X-ray structure of the TLR8-ectodomain homodimer:**1** complex indicates the weakly basic group forms an ionic interaction with Asp543 of one TLR8 monomer (Chain A, Figure 2A). The

lipophilic propyl chain extends into a narrow but deep hydrophobic pocket formed by residues Gly572, and Val573 from chain A, and Phe346, Tyr348, Gly376, Val378, Ile403, and Phe405 from chain B of the second TLR8 monomer. All the compounds in Figure 1 have a lipophilic group that likely occupies this pocket illustrating its importance for binding of small molecule agonists. The lipophilic pocket of TLR7 based on homology modeling was expected to be very similar to that of TLR8. Thus, the major structural differences between TLR7 and TLR8 within the ligand binding site, are residues Gly351 (Chain B) and Asp545 (Chain A), located at the front of the pocket (Figure 2A). These residues correspond to Gln354 and Leu557, respectively, in TLR7. Lead **6a** was modeled into the binding site of TLR8 to establish the same charged interaction with Asp543, and orientate the *N*-alkyl sidechain into the lipophilic pocket (Figure 2B). The model also suggested that the α-carbon of the alkyl sidechain was the most proximal atom from which to explore substitutions directed toward the front of the pocket in an attempt to engage Asp545 of TLR8. It was reasoned that polar groups could lead to a water mediated or direct hydrogen bond to Asp545 in TLR8, but would be unfavorable toward TLR7, due to presence of the lipophilic Leu557 sidechain, thereby generating TLR8 selectivity.

Figure 2. **A**. TLR8-Ectodomain:**1** X-ray complex with protons added to the ligand by modeling. Lighter green shading indicates Chain A surface of one TLR8 monomer and darker green is Chain B of the second TLR8 monomer; **B**. Model of **6a**; **C**. Model of (*R*)-**6d** with a bridging water hydrogen bond to Asp545; **D**. Model of (*R*)-**6d** with a direct hydrogen bond to Asp545; **E**. Cross section view of (*R*)-**6d** occupying the lipophilic pocket; **F**. Model of (*S*)-**6d** with a bridging water hydrogen bond to Asp545. All modeled compounds in **B-F** were docked into the TLR8 x-ray structure, PDB:3W3M

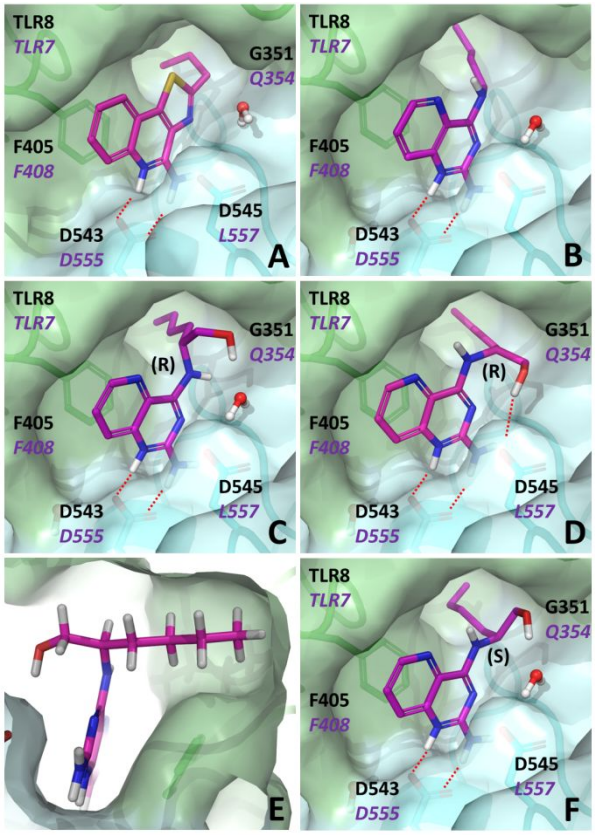

Scheme 1 illustrates the preparation of a variety of C-4 modified pyrido[3,2-*d*]pyrimidine compounds starting from the commercially available 2, 4-dichloropyrido[3,2-*d*]pyrimidine **8**. Nucleophilic addition of butan-1-ol or amines **11a-h** at C-4 was followed by addition of 2, 4-dimethoxybenzyl (Dmb) amine at C-2 to afford the intermediates **9** and **12a-h**. Acid deprotection of the Dmb group afforded the target compounds **10** and **6a-f**. Ester **12g** was reduced to the alcohol before Dmb removal to yield (*R*)-**6g**, and ester **12h** was first hydrolysed to the acid followed by Dmb removal to afford (*R*)-**6h**. The amides (*R*)-**6i** and (*R*)-**6j** were

generated from the above acid intermediate using a HATU mediated coupling prior to Dmb removal.

Scheme 1. Synthesis of N^4- and O^4-substituted pyrido[3,2-*d*]pyrimidin-2-amines[a]

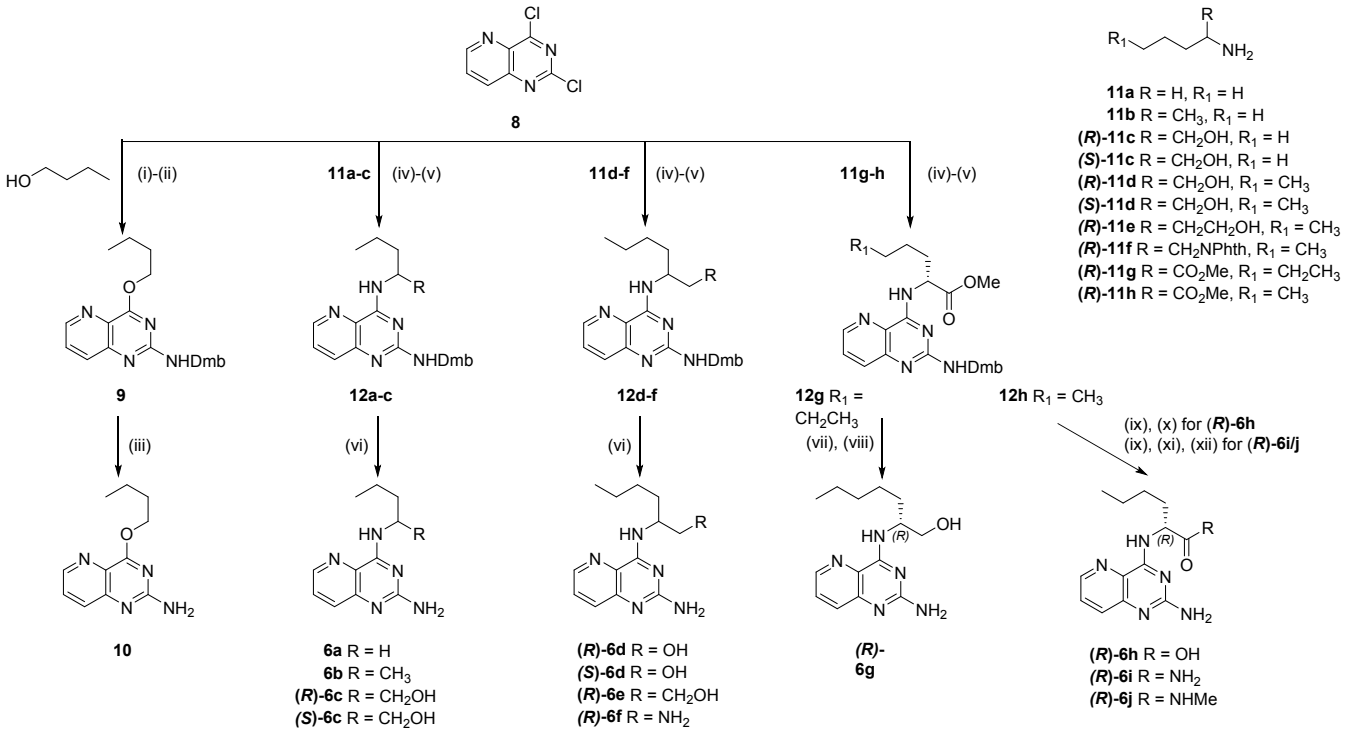

[a]Reagents and Conditions. (i) Butan-1-ol, NaH (60% disp.), 71%; (ii) 2,4-dimethoxybenzyl(Dmb)-NH_2, iPr_2NEt, 100°C, 37%; (iii) TFA, 9%; (iv) amine **11a-h**, iPr_2NEt; rt, (100°C for (*R*)-**11e**); (v) Dmb-NH_2, iPr_2NEt, 100-135°C, 52% for **12g**, 68% for **12h**; (vi) TFA, 11-73% over 3 steps; (vii) LAH; (viii) TFA, 5% over 2 steps; (ix) KOH(aq.), MeOH, quant.; (x) TFA, quant.; (xi) HATU, iPr_2NEt, NMP, ammonia (14%) or methylamine (18%); (xii) TFA, 22-42%.

Table 1. TLR activity of N^4- and O^4-substituted pyrido[3,2-*d*]pyrimidin-2-amines

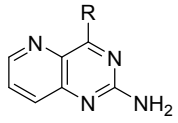

Cpd.	R	IL-12p40 EC_{50} (μM)[a]	IFN-α EC_{50} (μM)[a]
1 (3M-002)	-	4.9	18
3 (VTX 2337)	-	1.3	>30
10		>50	>50
6a		1.9	2.2
6b		3.1	5.1
(*R*)-6c	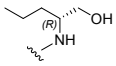	19	>50
(*S*)-6c	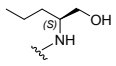	0.43	2.00
(*R*)-6d	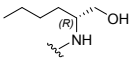	0.79	>50
(*S*)-6d	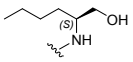	0.42	0.91
(*R*)-6e	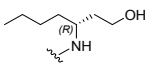	4.3	>50
(*R*)-6f	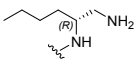	25	>50
(*R*)-6g	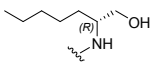	3.33	>20
(*R*)-6h	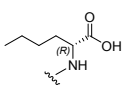	>50	>50
(*R*)-6i	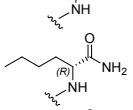	36	>50
(*R*)-6j	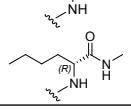	>50	>50

[a]Average of n ≥ 2 results

The induction of IL-12p40 (TLR8 cytokine) and IFN-α (TLR7 cytokine) in PBMCs for compounds **6a-j** is reported in Table 1. The lack of TLR activity for *O*[4]-linked analog **10** established that the corresponding amine linkage in **6a** was critical, and the similar potency of

the α-branched analog, **6b**, indicated that α-carbon branching was tolerated by both TLRs. Further extension of the α-branching group by the addition of a hydroxyl group resulted in 5-fold improved TLR8 potency and 5-fold selectivity for (*S*)-**6c** toward TLR8, whilst the corresponding (*R*)-**6c** isomer was 10-fold less potent toward TLR8. A significant advance was observed for isomers (*R*)-**6d** and (S)-**6d** that extend the α-alkyl chain to 4 carbons from the branch point. The (*S*)-**6d** isomer had comparable potency and selectivity to the shorter chain analog (*S*)-**6c**, but the (*R*)-**6d** isomer was > 20-fold more potent than (*R*)-**6c** toward TLR8 and had no TLR7 mediated IFN-α induction up to 50 μM, leading to the first selective TLR8 agonist in the series. Extending the α-alkyl chain with another methylene, analog (*R*)-**6g**, reduced potency while extending the hydroxyl group further from the branch point by one methylene, analog (*R*)-**6e**, was also less potent. Modification of the hydroxyl in (*R*)-**6d** to an amine, (*R*)-**6f,** or other groups capable of hydrogen bond donation e.g. **6h-j**, afforded only weak activity. Taken together, the SAR established that the length and *R* stereochemistry of the lipophilic sidechain in (*R*)-**6d**, together with the hydroxyl group were all required for optimal TLR8 potency and selectivity.

Modeling was used in an attempt rationalize the TLR8 potency SAR and also the differential selectivity toward TLR7 of the two isomers (*R*)-**6d** and (*S*)-**6d**. One pose for the (*R*)-**6d** analog in TLR8 (Figure 2C) suggested the hydroxyl was interacting via a water molecule with Asp545 and the N^4-alkyl group was rotated 180° relative to its orientation in **6a**. A second pose (Figure 2D) maintained the orientation of the N^4-alkyl group relative to **6a**, but led to the displacement of the bridging water molecule and the formation of a direct hydrogen bond to Asp545. Both possibilities were considered, but it wasn't until an x-ray co-crystal structure of compound (*R*)-**7** was solved that the direct hydrogen bond model was deemed to be correct (*vide infra*). Figure 2E shows a cross section of the lipophilic pocket with the 4 carbon chain of (*R*)-**6d**

fully occupying the space in the lipophilic pocket. The total distance from the end of the 4 carbon chain to the hydroxyl group is ideal to occupy the lipophilic pocket whilst also enabling the hydroxyl group to interact with Asp545. However, the shorter 3-carbon (*R*)-**6c** and longer 5-carbon (*R*)-**6g** lengths are suboptimal. The 5-fold weaker activity of (*R*)-**6e,** which has an identical length to (*R*)-**6d**, is presumed to be a combination of incomplete occupancy of the lipophilic pocket from the α-branch point and the greater entropic penalty of the more flexible hydroxyethyl group that forms the key interaction with Asp545. The (*S*)-**6d** isomer was modeled in TLR8 in a pose similar to **6a** and is presumed to derive its TLR8 potency from a similar water mediated interaction with Asp545 (Figure 2F). However, the fact that (*S*)-**6d** and indeed the shorter (*S*)-**6c** analog had comparable TLR7 and TLR8 potency is harder to rationalize, but does suggest that other binding poses are present in the TLR7 binding site that allow these *S*-isomers to generate favorable interactions with Leu557 despite the presence of the hydroxyl group. More thorough X-ray studies using TLR7 and TLR8 constructs will be required to tease out the binding modes of the *S* isomers in TLR7, the feasibility of which has now increased given the recent publication of TLR7 x-ray small molecule complex structures.[23]

The pyrido[3,2-*d*]pyrimidine heterocycle forms a π-stacking interaction with the aromatic ring of Phe405 (Figure 2A) so it was of interest to explore the effects of alternate heterocycle cores. The corresponding quinazolines of both **6d** isomers, (*R*)-**14** and (*S*)-**14**, and quinoline isomers, (*R*)-**16** and (*S*)-**16,** were therefore prepared according to Scheme 2. The quinazoline analogs have recently been shown to be TLR8 selective in HEK reporter assays.[24] Commercial **13** was converted to isomers **14** via a BOP mediated coupling with the amine isomers **11d,** while the corresponding quinolines **16** were prepared in a palladium cross coupling of quinoline **15** with amine isomers **11d**.

Scheme 2. Synthesis of N^4-substituted quinazoline-2-amines, **14**, and quinoline-2-amines, **16**[a]

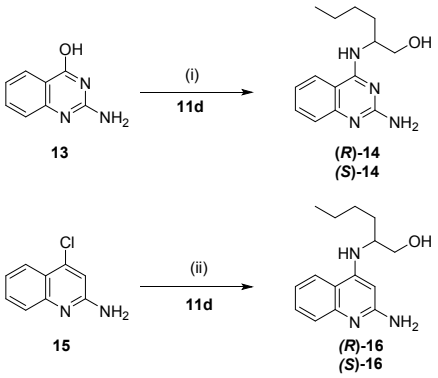

[a]Reagents and Conditions. (i) DMF, DBU, BOP, **11d**, 62-71%; (ii) $Pd(dba)_2$, NaO^tBu, (*R*)-BINAP, **11d**, 135°C, 7-16%.

Table 2. TLR activity of N^4-substituted quinazolin-2-amines and quinolin-2-amines

Cpd.	Structure	IL-12p40 EC_{50} (μM)[a]	IFN-α EC_{50} (μM)[a]
(*R*)-**14**	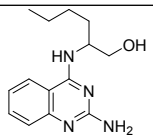	1.84	>50
(*S*)-**14**		0.71	0.57
(*R*)-**16**	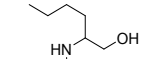	>50	>50
(*S*)-**16**	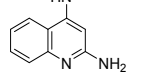	>50	>50

[a]Average of n≥2 results

The quinazoline isomers **14** had parallel SAR to their corresponding pyrido[3,2-*d*]pyrimidin-2-amines albeit 2-fold less potent in each case toward TLR8 (Table 2). In contrast removal of the additional nitrogen in the core, quinolines **16**, resulted in complete loss of activity. The measured pKa for (*R*)-**6d** was 7.0, 8.2 for quinazoline (*R*)-**14**, and calculated to be even higher for the quinoline (*R*)-**16**[25], thus protonation state in the endosome was not the cause of lower activity. This loss of activity for the quinoline (*R*)-**16** is also surprising in light of the

observation that quinoline **2**, is a potent TLR8 agonist, and suggests that the 2-aminoquinoline core binds differently to these other cores in the TLR8 pocket leading to suboptimal positioning of the N^4-group into the lipophilic pocket.

Cytotoxicity screening of the TLR8 selective lead (*R*)-**6d** indicated a narrow cell-based toxicity index, ~10-fold (MT-4 CC_{50}/IL-12p40 EC_{50}) in the rapidly proliferating MT-4 cell line due to 'off-target' effects. Continued optimization was therefore conducted and focused on exploring substitution at the remaining α-carbon position leading to α, α-substituted analogs. In the models of (*R*)-**6d** and (*S*)-**6d** (Figures 2C, 2D) there is a small unoccupied space near the unsubstituted α-site. To support this effort several chiral α, α-substituted amino acid esters and alcohols were required and their preparation is described in Scheme 3. The amino acid esters **18a-b** and **18g** were generated from commercially available unnatural amino acids through esterification of the acid followed by protecting group removal as needed. The tertiary amino alcohol (*S*)-**18c** was derived from the acid (*S*)-**19** via a borane reduction, and alcohols (*R*)-**18c**-**f** by stereospecific synthesis from the 5,6-dihydro-2*H*-1,4-oxazin-2-one intermediate (*R*)-**20**.[26] The oxazin-2-one route not only facilitated control of stereochemistry, but also allowed for rapid generation of amino alcohols with modified alkyl chains e.g. (*R*)-**18f**.

Scheme 3. Stereoselective synthesis of α, α-substituted amino acid esters and alcohols[a]

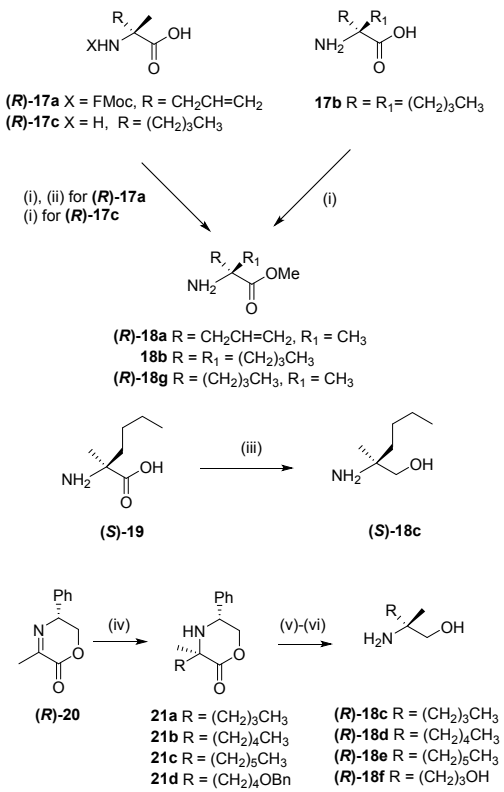

[a]Reagents and Conditions. (i) $TMSCHN_2$, MeOH, quant.; (ii) Piperidine, THF, 85% over 2 steps; (iii) $BH_3 \cdot THF$; (iv) $BF_3 \cdot OEt_2$, -78°C, RMgCl, 60-76% (v) $LiBH_4$, 0°C-rt, quant.; (vi) $Pd(OH)_2/C$, EtOH, HCl, H_2, 70-75°C, quant.

The subsequent coupling of the α, α-substituted amines to the pyrido[3,2-*d*]pyrimidine-2-core **8** is described in Scheme 4. Unlike the mono α-substituted series the more hindered α, α-substituted amines typically required elevated temperatures in the nucleophilic substitution reaction. In examples where Dmb protecting groups were present, their removal proceeded as described previously, along with any ester or carbon-carbon double bond reductions, to afford **23a-e**. The same methods were also applicable to the nucleophilic substitution on the 7-F and 7-Cl heterocycle intermediates, **25** and **27** respectively. 7-Chloro intermediate **28** could also be converted to the 7-methyl analog (*R*)-**30** using methylboronic acid in a Suzuki cross coupling.

Finally, preparation of (*S*)-**7** illustrates, an alternative approach to 7-fluoro analogs via a simple two step method from readily available fluoropicolinic acid **31**.

Scheme 4. Synthesis of N^4-α, α-substituted pyrido[3,2-*d*]pyrimidin-2-amines[a]

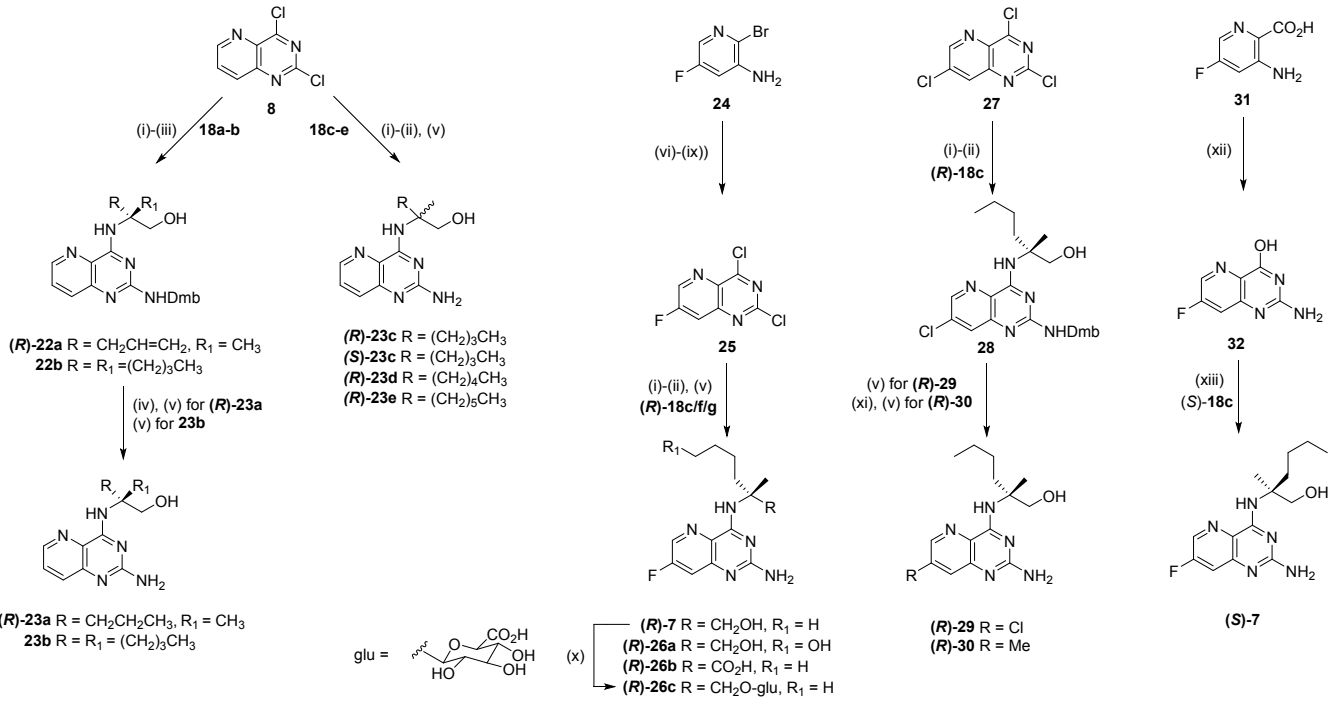

[a]Reagents and Conditions. (i) amine **18a-e**, iPr_2NEt, 80°C; (ii) Dmb-NH_2, iPr_2NEt (K_2CO_3 for (*R*)-**23e** and (*R*)-**26a**), 85-120°C, 17-66% over 2 steps; (iii) LAH, 29-100%, (over 2 steps, (*R*)-**23a** (45%) and (*R*)-**30** (82%); over 3 steps (*S*)-**23c** (26%) and (*R*)-**23d** (7%)); (iv) Pd/C, H_2;(v) TFA, 7%-quant.; (vi) $Pd(Ph_3)_4$, $ZnCN_2$, DMF, 115°C, quant.; (vii) K_2CO_3, H_2O_2, 0°C, 97% over 2 steps; (viii) $(COCl_2)_3$, 110°C, 90%; (ix) PCl_5, $POCl_3$, 110°C, 75%; (x) Fermentation; (xi) $CH_3B(OH)_2$, $Pd(Ph_3)_4$, K_3PO_4, 150°C; (xii) $ClC(=NH)\text{-}NH_2$, $(CH_3)_2SO_2$, 160°C, 24%; (xiii) NMP, BOP, DBU, (*S*)-**18c**, 20%.

Table 3. N^4-α, α-substituted pyrido[3,2-*d*]pyrimidin-2-amines

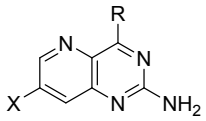

Cpd.	R	X	IL-12p40 EC_{50} (μM)[a]	IFNα EC_{50} (μM)[a]	MT-4 CC_{50} (μM)[a]	CC_{50} Index	pKa	Log D	Caco-2 (10^{-6} cms^{-1})	MS r/d/c/h CL pred. (L/h/kg)
(*R*)-**6d**	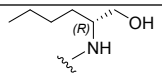	H	0.79	>50	7.8	10	6.8	-	-	-
(*R*)-**23a**	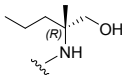	H	2.4	>50	>50	>21	-	1.1	-	-
23b	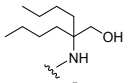	H	>50	>50	38	-	-	2.9	-	-
(*R*)-**23c**	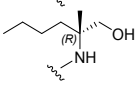	H	0.17	15	31	182	-	1.4	29/29	3.5/1.4/1.3/0.8
(*S*)-**23c**	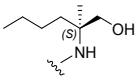	H	2.4	7.9	26	11	-	1.4	32/31	3.5/1.5/1.4/0.8
(*R*)-**23d**	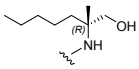	H	0.58	20	17	29	-	1.8	-	-
(*R*)-**23e**	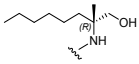	H	10	>50	3.6	0.4	-	2.5	-	-
(*S*)-**7**	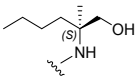	F	3.3	>50	0.79	0.2	-	-	-	-
(*R*)-**7**	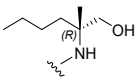	F	0.22	>50	17	77	6.3	2.0	7.9/11	3.0/1.7/1.5/1.0
(*R*)-**26a**	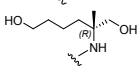	F	>50	>50	>50	-	-	-	-	-
(*R*)-**26b**	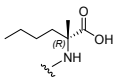	F	>50	>50	>50	-	-	-	-	-
(*R*)-**26c**	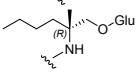	F	>50	>50	>50	-	-	-	-	-
(*R*)-**29**	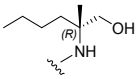	Cl	0.27	>42	22	81	6.4	2.6	32/31	3.4/1.8/1.4/1.0
(*R*)-**30**	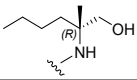	Me	0.16	>50	23	144	7.1	1.9	31/29	3.8/1.1/1.5/0.5

[a]Average of n≥2 results. Cytotoxicity (CC_{50}) index, defined as MT-4 CC_{50} / IL-12p40 PBMC EC_{50}; AB, apical to basolateral; BA, basolateral to apical; MS, microsomes; r, rat; d, dog; c, cyno; h, human; CL pred., predicted clearance.

The α, α-substituted analogs **23a-e** were evaluated across a wide range of assays including TLR8 potency and selectivity, cytotoxicity index CC_{50} (MT-4 CC_{50} / IL-12p40 EC_{50}), pKa, log D, caco-2 cell permeability and in vitro microsomal metabolism (Table 3). The α-

methyl analog (*R*)-**23c**, not only improved the TLR8 potency by 5-fold compared to the corresponding mono α-substituted analog (*R*)-**6d**, but also retained >80-fold selectivity over TLR7, and improved the MT-4 cytotoxicity window to 182-fold. The *S* isomer, (*S*)-**23c** was >10-fold less active toward TLR8 than (*R*)-**23c** and less selective over TLR7 reinforcing the preference for the *R* isomer series. Like the previous mono α-substituted series, extending the α-alkyl chain analogs, (*R*)-**23d/e**, or shortening, (*R*)-**23a,** was less potent although the one methylene extended (*R*)-**23d** was only 3-fold less potent. The achiral analog **23b** was devoid of activity suggesting the second α-substitutent needs to be sterically small, consistent with the modeling prediction.

Turning attention to the pharmacokinetic properties, the low molecular weight, moderate logD, and good solubility in aqueous media resulted in excellent passive permeability in caco-2 cells for both (*R*)- and (*S*)-**23c** with no apparent efflux ratio (efflux ratio = BA/AB). High first pass clearance was predicted using microsomal incubations for both **23c** isomers from multiple preclinical species. Metabolite identification studies in hepatocytes indicated extensive heterocycle core metabolism which raised the concern that some of the oxidized core metabolites could be immunologically active in vivo, leading to a convoluted in vivo profile. Therefore, in an attempt to suppress core metabolism, the core was modified at several positions of which the most favorable was 7-substitution, analogs (*R*)-**7 (**7-F**)**, (*R*)-**29** (7-Cl) and (*R*)-**30** (7-Me) respectively. The pKa of the heterocycle nitrogen was lowered by only 0.5 units for the 7-F and 7-Cl analogs to a range of 6.3-7.1, higher than the endosome, and therefore not expected to impact potency (Table 3). Indeed, all three analogs demonstrated comparable potency to the 7-unsubstituted analog (*R*)-**23c**, but TLR8 selectivity improved to >185 fold, and the CC_{50} index in the MT-4 cell line was >77-fold. No significant changes in permeability or the predicted

clearance across species was noted except for a lower predicted human clearance of the C7-methyl analog (*R*)-**30**. The risk of potentially lower first pass clearance for this analog was sufficient to rule it out of contention for selection. Metabolite identification following incubation of (*R*)-**7** in human hepatocytes indicated that core oxidation had indeed been suppressed and the most dominant metabolites were lipophilic chain oxidation, hydroxyl oxidation to the acid, and glucuronidation. Although the specific site of oxidation on the lipophilic chain was not rigorously identified, the SAR for small changes along this chain was extremely narrow, and even small changes such as fluorine led to weaker activity (data not shown). Although it was extremely unlikely oxidation along the four carbon chain would result in an active metabolite, the terminal hydroxyl (*R*)-**26a** was prepared and tested as one potential metabolite to verify lack of TLR7/8 activity (Table 3). The acid (*R*)-**26b** was also prepared and found to be inactive to both TLRs, as was the *O*-glucuronide (*R*)-**26c** that was structurally confirmed by NMR following isolation from microbial fermentation mixtures. Compound (*R*)-**7** sufficiently de-risked the potential metabolite concerns and was more potent than (*R*)-**29** so it was selected for in vivo evaluation. In each non-clinical species, high clearance and low oral bioavailability was observed consistent with the in vitro prediction of high first pass metabolism (Table 4). A bile duct cannulated study in rat detected minimal parent compound in bile and urine, confirming metabolism was the dominant mechanism of clearance in rat. Oral absorption was confirmed through analysis of portal vein samples in dog and cynomolgus monkey following oral dosing, and these data indicated at least 28% absorption in dog and ~100% in cynomolgus monkey. Taken together, the in vitro predictions of good oral absorption and high first pass clearance were confirmed in vivo in the non-clinical species. The predicted first pass clearance of (*R*)-**7** in

humans is high, close to that of liver blood flow, so (*R*)-**7** was expected to be a well absorbed high clearance compound in humans meeting the desired target profile (Table 3).

Table 4. Mean plasma pharmacokinetic parameters of (*R*)-**7** following IV and oral administration

	IV[1]			Oral[2]		
Species	CL (L/h/kg)	V_{ss} (L/kg)	$t_{½}$ (h)	AUC_{inf} (nM•h)	C_{max} (nM)	F
Sprague Dawley Rat	1.8 ± 0.2	1.1 ± 0.0	1.45 ± 0.12	827 ± 540	517 ± 224	8.8% ± 5.7%
Beagle Dog	1.2 ± 0.13	1.01 ± 0.13	1.32 ± 0.18	11.8 ± 7.3	9.7 ± 7.7	0.8% ± 0.5%
Cynomolgus Monkey	6.2 ± 1.8	2.1 ± 1.5	0.67 ± 0.07	4.7 ± 4.2	1.2 ± 0.5	0.3% ± 0.2%

[1]30-min intravenous infusion to Sprague Dawley (SD) rats (1 mg/kg), beagle dogs (0.25 mg/kg) and cynomolgus monkeys (0.1 mg/kg) (mean ± SD, n = 3). [2]Oral administration to SD rats (5 mg/kg), beagle dogs (0.5 mg/kg) and cynomolgus monkeys (3 mg/kg), formulation was 2% ethanol, 40% PEG 300 and 58% 0.01N HCl.

Evidence for direct binding of (*R*)-**7** to TLR8 was attained by solving the ectodomain TLR8:(*R*)-**7** co-crystal structure (Figure 3). The structure indicates that the compound binds with a direct hydrogen bond to Asp545, the basic group interacts with Asp543, and the lipophilic N^4-alkyl chain occupies the narrow lipophilic pocket. However, Asp545 shifted slightly relative to the published structure of **1** to provide a more optimal direct hydrogen bond to the hydroxyl group of (*R*)-**7.** This supports the premise that the Asp545 interaction is the key driver of TLR8 potency and selectivity. The α-methyl group is directed to the top of the binding site and nicely occupies the space proximal to Tyr348, Val378 and Gly351 which results in increased binding potency.

Figure 3. Single co-crystal structure of TLR8 ectodomain:(*R*)-**7** complex. PDB Code: 6WML

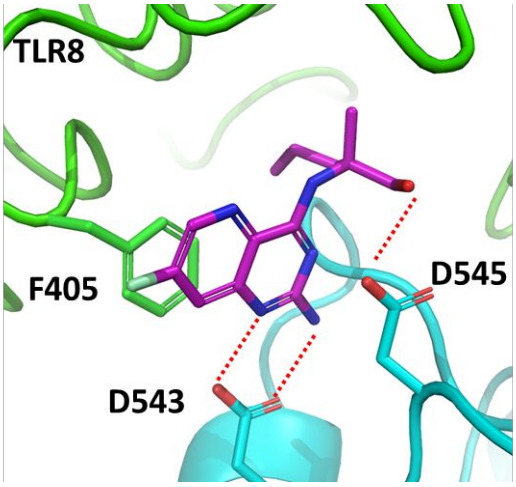

The broader selectivity profile of (*R*)-**7** toward immune receptors was assessed in reporter gene assays using HEK293 cells, stably expressing individual human TLRs or other innate immune receptors. The minimum effective concentration (MEC) of (*R*)-**7** that resulted in a 3-fold increase above background was 49 nM for human TLR8 (Figure 4). In contrast, the MEC for human TLR7 was 5197 nM further supporting a mechanism of selective engagement of (*R*)-**7** on human TLR8 over human TLR7. Moreover, (*R*)-**7** did not stimulate HEK293 cells stably expressing other human TLRs including TLR2, TLR3, TLR4, TLR5, TLR9 and other receptors including Nod-like receptors (NLRs; NOD1 and NOD2), RIG-I -like receptors (RLRs; RIG-I and MDA5) or C-type lectin receptors (CLRs; Dectin1a, Dectin 1b and Mincle) (data not shown). This data, taken together with the structural data, supports the direct and selective engagement and activation of TLR8 by (*R*)-**7**.

Figure 4. TLR8 and TLR7 HEK293 reporter assay response to (*R*)-**7**

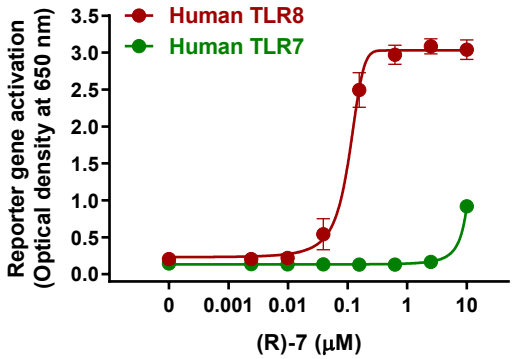

In HBV-infected PHH viral RNAs are transcribed from the viral genome (covalent closed circular DNA, cccDNA) leading to the expression of the viral proteins e.g. HBeAg and HBsAg. Direct stimulation of HBV infected PHH with (*R*)-**7** did not result in any antiviral effects consistent with the lack of robust TLR8 expression in human hepatocytes (data not shown). In an indirect experiment, designed to assess the antiviral effect of TLR8 induced immune mediators generated in PBMCs, HBV-infected PHH were treated with media from human PBMCs stimulated with (*R*)-**7** ((*R*)-**7**-CM). Exposure of HBV-infected PHH to (*R*)-**7**-CM over 10 days resulted in a decrease in HBV, DNA HBV RNA, HBeAg and HBsAg levels by >50% relative to no compound control (Figure 5). However, (*R*)-**7**-CM did not reduce levels of cccDNA demonstrating that, in this in vitro system, TLR8-induced cytokines are insufficient to induce non-cytolytic degradation of cccDNA (data not shown).

Figure 5. Antiviral activity in HBV-infected PHH treated with (*R*)-**7**-CM.

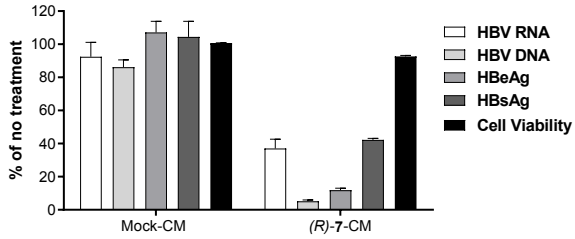

The woodchuck hepatitis virus (WHV) is a hepadnavirus closely related to HBV and therefore the woodchuck model has been used to evaluate TLR agonists.[27] The TLR7 agonist vesatolimod (GS-9620) demonstrated anti-WHV activity in the woodchuck model prompting this program to conduct a similar model to evaluate oral (*R*)-**7** following local IACUC guidelines. The results from oral dosing of (*R*)-**7** have recently been published and will only be summarized here.[28] Once weekly oral dosing of (*R*)-**7** at 3 mg/kg for 8 weeks reduced serum WHV DNA and WHBsAg to below the limit of detection in 3 out of 6 treated woodchucks. These responses were not conclusively associated with baseline levels of WHV DNA or WHBsAg. The responses were sustained following cessation of dosing in these 3 animals. Strikingly, >95% reductions in intrahepatic WHV RNA, WHV DNA and WHV cccDNA were also observed in these 3 sustained antiviral responders. Pharmacokinetic sampling was limited during the study to a single timepoint at 0.5 h following dosing. There was a trend to higher exposures in the responding animals in this study but this trend was not reproduced in a larger follow-on study.[28] The lack of a clear correlation between systemic drug exposure and efficacy suggests that the response is not driven from systemic activation of TLR8 but more likely, pre-systemic gut and liver TLR8 activation. Understanding the molecular basis for the differential responses in woodchucks is now the focus of future experiments.[28] In conclusion this striking result observed in several woodchucks strongly supports the potential for (*R*)-**7** to be an effective new agent for the treatment of CHB.

Conclusion

The clinical compound (*R*)-**7** is an orally active selective TLR8 agonist, that was discovered through structure guided evolution of the C-4 substituent on an initial pyrido[3,2-*d*]pyrimid-2-

amine lead. (*R*)-**7** demonstrated EC_{50}=220 nM for induction of IL-12p40 in cryopreserved human PBMCs and >100-fold selectivity for TLR8 against TLR7 in PBMCs and HEK293 cells. In vivo, (*R*)-**7** demonstrated good oral absorption properties across several preclinical species and a high first pass clearance that limited systemic exposure levels. Treatment of HBV-infected PHH with cytokines obtained from (*R*)-**7**-stimulated PBMCs decreased the levels of HBV DNA and RNA in addition to other viral proteins. These findings combined with the promising in vivo efficacy in the woodchuck model of CHB, supports the potential of (*R*)-**7** to be an effective new treatment option for CHB. (*R*)-**7** is currently in multiple phase 2 studies for the treatment of CHB.

Experimental Section

All organic compounds were synthesized at Gilead Sciences, Inc. (Foster City, CA) unless otherwise noted. Commercially available solvents and reagents were used as received without further purification. Nuclear magnetic resonance (NMR) spectra were recorded on a Varian Mercury Plus 400 MHz at room temperature, with tetramethylsilane as an internal standard. Proton nuclear magnetic resonance spectra are reported in parts per million (ppm) on the δ scale and are referenced from the residual protium in the NMR solvent ($CHCl_3$-d_1: δ 7.26, MeOH-d_4: δ 3.31, DMSO-d_6: δ 2.50, CH_3CN-d_3: δ 1.94). Data is reported as follows: chemical shift (multiplicity [s = singlet, d = doublet, t = triplet, q = quartet, p = pentet, h = heptet, m = multiplet, br = broad, app = apparent], coupling constants (*J*) in Hertz, integration). See Supporting Information for NMR spectra of final compounds. Preparative normal phase silica gel chromatography was carried out using a Teledyne ISCO CombiFlash Companion instrument with silica gel cartridges. Preparative HPLC purification is described in the experimental

method. Purities of the final compounds were determined by analytical high-performance liquid chromatography (HPLC), and were greater than 95% unless otherwise noted (See Supporting Information for HPLC spectra and methods). LC/MS was conducted on a Thermo Finnigan MSQ Std using electrospray positive and negative $[M+1]^+$ and $[M-1]^-$, and a Dionex Summit HPLC System (model: P680A HPG) equipped with a Gemini 5 μ C18 110A column (30 mm × 4.60 mm), eluting with CH_3CN containing 0.1% formic acid, and water containing 0.1% formic acid; 0 min-1.8 min 2-100% CH_3CN, 1.8 min-1.85 min 100%-2% CH_3CN, 1.85 min-2.00 min 2% CH_3CN at 1800μL/min.

CAUTION: The compounds generated using these methods are potent immunomodulators and should be handled with appropriate personal protective equipment practices, including double glove, lab coat disposable arm bands, and disposable footwear booties. A full mask respirator should be used when handling the solid form of the compounds in amounts exceeding 10 mg.

The synthesis, characterization data, and associated references for the amines **11e-g** and **18a-g** are provided in supporting information.

***N*^{4}-butylpyrido[3,2-*d*]pyrimidine-2,4-diamine (6a).** Compound **8** (CAS# 39551-54-7, Astatech, Inc., Bristol, PA) (50 mg, 0.25 mmol) in THF (2 mL) was treated with butan-1-amine **11a** (0.03 mL, 0.28 mmol) and *N,N*-diisopropylethylamine (0.13 mL, 0.75 mmol). The mixture was stirred for 30 min and then Dmb-NH_2 (0.19 mL, 1.25 mmol) and *N*,*N*-diisopropylethylamine (0.13 mL, 0.75 mmol) were added. The mixture was heated at 100°C for 16 h, cooled to rt, diluted with EtOAc (20 mL), washed with water (20 mL), brine (20 mL), and then concentrated under reduced pressure. The residue was subjected to silica gel chromatography eluting with 0-100% EtOAc-hexanes to provide **12a**. LC/MS (*m/z*) 368.14 [M+1]. **12a** was treated with TFA (3

mL), stirred for 30 min, diluted with water and MeOH and then stirred for a further 60 min. The mixture was then concentrated under reduced pressure and the residue co-evaporated with MeOH (3 x). The solid was collected by filtration to provide **6a** (51 mg, 62%) as a TFA salt. ^{1}H NMR (400 MHz, MeOH-d_4) δ 8.59 (dd, J = 4.4, 1.4 Hz, 1H), 7.82 (dd, J = 8.5, 1.4 Hz, 1H), 7.72 (dd, J = 8.4, 4.4 Hz, 1H), 3.66 (t, J = 7.3 Hz, 2H), 1.76 – 1.64 (m, 2H), 1.43 (dq, J = 14.7, 7.4 Hz, 2H), 0.98 (t, J = 7.4 Hz, 3H). LC/MS (*m/z*) 218.1 [M+1].

***N*^{4}-(pentan-2-yl)pyrido[3,2-*d*]pyrimidine-2,4-diamine (6b).** The same procedure as **6a,** except replacing **11a** with (+/-)-pentan-2-amine **11b,** provided **6b** (63 mg, 73 %) as a TFA salt. ^{1}H NMR (400 MHz, MeOH-d_4) δ 8.61 (dd, J = 4.4, 1.4 Hz, 1H), 7.84 (dd, J = 8.5, 1.4 Hz, 1H), 7.74 (dd, J = 8.5, 4.4 Hz, 1H), 4.60 – 4.45 (m, 1H), 1.74 (dtd, J = 13.5, 8.3, 6.7 Hz, 1H), 1.68 – 1.55 (m, 1H), 1.41 (app h, J = 7.5 Hz, 2H), 1.32 (d, J = 6.6 Hz, 3H), 0.95 (t, J = 7.4 Hz, 3H). LC/MS (*m/z*) 232.1 [M+1].

(*R*)-2-((2-aminopyrido[3,2-*d*]pyrimidin-4-yl)amino)pentan-1-ol ((*R*)-6c). The same procedure as **6a,** except replacing **11a** with (*R*)-2-aminopentan-1-ol (*R*)-**11c,** provided (*R*)-**6c** (40 mg, 36 %) as a TFA salt. ^{1}H NMR (400 MHz, MeOH-d_4) δ 8.64 (dd, J = 4.4, 1.4 Hz, 1H), 7.83 (dd, J = 8.5, 1.5 Hz, 1H), 7.76 (dd, J = 8.5, 4.4 Hz, 1H), 4.55 (dq, J = 7.4, 5.4 Hz, 1H), 3.78 – 3.69 (m, 2H), 1.77 – 1.65 (m, 2H), 1.52 – 1.36 (m, 2H), 0.98 (t, J = 7.3 Hz, 3H). LC/MS (*m/z*) 248.1 [M+1].

***(S)*-2-((2-amino-[3,2-*d*]pyrimidin-4-yl)amino)pentan-1-ol ((*S*)-6c).** The same procedure as **6a,** except replacing **11a** with (*S*)-2-aminopentan-1-ol (*S*)-**11c,** provided (*S*)-**6c** (3 mg, 11 %) as a TFA salt with the exception that, after the addition of the Dmb-NH_2 the mixture was heated at 135 ℃ in a microwave reactor for 30 min and the final compound (*S*)-**6c** was subjected to purification via reverse phase preparative HPLC (10-70% CH_3CN in water with

0.1% TFA using a Hydro-RP column over a 20 min gradient). ^{1}H NMR (400 MHz, MeOH-d_4) δ 8.37 (dd, J = 4.2, 1.5 Hz, 1H), 7.62 (dd, J = 8.5, 1.5 Hz, 1H), 7.52 (dd, J = 8.5, 4.2 Hz, 1H), 4.37 (dq, J = 10.1, 5.0 Hz, 1H), 3.69 (d, J = 4.9 Hz, 2H), 1.78 – 1.62 (m, 2H), 1.44 (dq, J = 14.5, 6.9 Hz, 2H), 0.97 (t, J = 7.3 Hz, 3H). LC/MS (*m/z*) 248.2 [M+1].

(*R*)-2-((2-aminopyrido[3,2-*d*]pyrimidin-4-yl)amino)hexan-1-ol ((*R*)-6d). The same procedure as **6a,** except replacing **11a** with (*R*)-2-aminohexan-1-ol (*R*)-**11d,** provided (*R*)-**6d** (50 mg, 55 %) as a TFA salt. ^{1}H NMR (400 MHz, MeOH-d_4) δ 8.64 (dd, J = 4.3, 1.5 Hz, 1H), 7.82 (dd, J = 8.5, 1.5 Hz, 1H), 7.77 (dd, J = 8.5, 4.3 Hz, 1H), 4.53 (m, 1H), 3.73 (d, J = 5.3 Hz, 2H), 1.85 – 1.59 (m, 2H), 1.39 (m, 4H), 0.91 (m, 3H). LC/MS (*m/z*) 262.2 [M+1].

***(S)*-2-((2-aminopyrido[3,2-*d*]pyrimidin-4-yl)amino)hexan-1-ol ((*S*)-6d).** The same procedure as **6a,** except replacing **11a** with (*S*)-2-aminohexan-1-ol (*S*)-**11d,** provided (*S*)-**6d** (46 mg, 50 %) as a TFA salt. ^{1}H NMR (400 MHz, MeOH-d_4) δ 8.63 (dd, J = 4.4, 1.4 Hz, 1H), 7.84 (dd, J = 8.5, 1.4 Hz, 1H), 7.76 (dd, J = 8.5, 4.4 Hz, 1H), 4.53 (m, 1H), 3.73 (d, J = 5.3 Hz, 2H), 1.87 – 1.61 (m, 2H), 1.52 – 1.31 (m, 4H), 1.01 – 0.85 (m, 3H). LC/MS (*m/z*) 262.2 [M+1].

(*R*)-3-((2-aminopyrido[3,2-*d*]pyrimidin-4-yl)amino)heptan-1-ol ((*R*)-6e). The same procedure as **6a,** except replacing **11a** with (*R*)-3-aminoheptan-1-ol (*R*)-**11e,** and heating at 100° for 1 h prior to the Dmb-NH_2 addition, provided (*R*)-**6e** (19 mg, 19%) as a TFA salt. ^{1}H NMR (400 MHz, MeOH-d_4) δ 8.63 (dd, J = 4.4, 1.5 Hz, 1H), 7.82 (dd, J = 8.5, 1.5 Hz, 1H), 7.76 (dd, J = 8.5, 4.4 Hz, 1H), 4.65 – 4.62 (m, 1H), 3.72 – 3.59 (m, 2H), 1.99 – 1.83 (m, 2H), 1.81 – 1.66 (m, 2H), 1.46 – 1.29 (m, 4H), 0.97 – 0.82 (m, 3H). LC/MS (*m/z*) 276.1 [M+1].

(*R*)-N^4-(1-aminohexan-2-yl)pyrido[3,2-*d*]pyrimidine-2,4-diamine ((*R*)-6f). The same procedure as **6a,** except replacing **11a** with (*R*)-**11f** and heating the reaction after the Dmb-NH_2

addition at 125°C for 24 h**,** provided (*R*)-**6f** (6 mg, 40 %) as a TFA salt. ^{1}H NMR (400 MHz, MeOH-d_4) δ 8.68 (dd, *J* = 4.4, 1.4 Hz, 1H), 7.89 (dd, *J* = 8.5, 1.5 Hz, 1H), 7.81 (dd, *J* = 8.5, 4.4 Hz, 1H), 7.24 (d, *J* = 8.3 Hz, 1H), 6.62 (d, *J* = 2.4 Hz, 1H), 6.55 (dd, *J* = 8.3, 2.4 Hz, 1H), 3.70 – 3.51 (m, 1H), 1.74 (ddh, *J* = 21.4, 14.1, 7.5 Hz, 2H), 1.63 – 1.30 (m, 4H), 0.98 (t, *J* = 7.1 Hz, 3H). LC/MS (*m/z*) 261.1 [M+1].

(*R*)-2-((2-aminopyrido[3,2-*d*]pyrimidin-4-yl)amino)heptan-1-ol ((*R*)-6g). Compound **8** (89 mg, 0.44 mmol) in THF (5 mL) was treated with *N,N*-diisopropylethylamine (0.26 mL, 1.76 mmol) and (*R*)-**11g** (71 mg, 0.44 mmol). The reaction was stirred for 1 h and then the mixture was treated with Dmb-NH_2 (0.17 mL, 1.1 mmol) and heated at 120℃ overnight. The reaction mixture was then partitioned between EtOAc (50 mL) and H_2O (50 mL). The organic layer was separated, dried, and concentrated under reduced pressure. The residue was subjected to silica gel chromatography eluting with 0-100% EtOAc-hexanes to provide the Dmb-intermediate **12g** (82 mg, 52%). LC/MS (*m/z*) 454.6 [M+1]. **12g** (169 mg, 0.37 mmol) was dissolved in THF (5 mL) and treated with 1M lithium aluminum hydride in Et_2O (1.1 mL, 1.1 mmol). The reaction mixture was stirred at rt for 2 h and then quenched with water. The mixture was extracted with EtOAc (3 x), the organics combined, dried, and concentrated under reduced pressure. The crude product (~20 mg) was used without further purification. LC/MS (*m/z*) 426.4 [M+1]. The crude product was dissolved in CH_2Cl_2 (2 mL) and TFA (0.5 mL) and the mixture stirred for 3 h. The reaction mixture was concentrated under reduced pressure and the residue subjected to reverse phase preparative HPLC (10-70% CH_3CN in water with 0.1% TFA using a Hydro-RP column over a 20 min gradient) to provide (*R*)-**6g** (0.7 mg, 5%) as a TFA salt. ^{1}H NMR (400 MHz, MeOH-d_4) δ 8.65 (dd, *J* = 4.3, 1.6 Hz, 1H), 7.92 – 7.66 (m, 2H), 4.66 – 4.43

(m, 1H), 3.73 (d, *J* = 5.3 Hz, 2H), 1.81 – 1.57 (m, 2H), 1.51 – 1.20 (m, 6H), 0.89 (t, *J* = 7.0 Hz, 3H). LC/MS (*m/z*) 276.4 [M+1].

(*R*)-2-((2-aminopyrido[3,2-*d*]pyrimidin-4-yl)amino)hexanoic acid ((*R*)-6h). Compound **8** (500 mg, 2.50 mmol) in THF (10 mL) was treated with *D*-norleucine, methyl ester hydrochloride (*R*)-**11h** (455 mg, 2.50 mmol, Combi-Blocks, Inc., San Diego, CA) and *N,N*-diisopropylethylamine (1.3 mL, 7.50 mmol). The mixture was stirred for 3.5 min and then Dmb-NH_2 (1.9 mL, 12.5 mmol), *N,N*-diisopropylethylamine (1.3 mL, 7.50 mmol), and THF (5 mL) were added. The mixture was heated to 100°C for 16 h, cooled to room temperature, diluted with EtOAc (50 mL), washed with water (50 mL), brine (50 mL), dried over Na_2SO_4, and concentrated under reduced pressure. The residue was subjected to silica gel chromatography eluting with 0-100% EtOAc-hexanes to provide methyl (*R*)-2-((2-((2,4-dimethoxybenzyl)amino)pyrido[3,2-*d*]pyrimidin-4-yl)amino)hexanoate **12h** (750.7 mg, 68%). ^{1}H NMR (400 MHz, $CHCl_3$-d_1) δ 8.33 (dd, *J* = 4.2, 1.5 Hz, 1H), 7.68 (d, *J* = 7.6 Hz, 1H), 7.43 (dd, *J* = 8.5, 4.2 Hz, 1H), 7.28 (s, 1H), 6.46 (d, *J* = 2.3 Hz, 1H), 6.41 (dd, *J* = 8.2, 2.4 Hz, 1H), 4.88 (q, *J* = 7.3 Hz, 1H), 4.59 (d, *J* = 6.0 Hz, 2H), 3.85 (s, 3H), 3.79 (s, 3H), 3.75 (s, 3H), 2.04 – 1.95 (m, 1H), 1.88 (dq, *J* = 14.8, 7.6 Hz, 1H), 1.40 (m, 4H), 0.91 (t, *J* = 7.1 Hz, 3H). LC/MS (*m*/*z*) 440.19 [M+1].

Methyl (*R*)-2-((2-((2,4-dimethoxybenzyl)amino)pyrido[3,2-*d*]pyrimidin-4-yl)amino)hexanoate **12h** (750.7 mg, 1.71 mmol) in THF (3.6 mL) and MeOH (3.6 mL) was treated with 1M aq. KOH (3.6 mL) and the mixture stirred for 4 h. The reaction was neutralized with 1 M aq. HCl and then concentrated under reduced pressure to provide (*R*)-2-((2-((2,4-dimethoxybenzyl)amino)pyrido[3,2-*d*]pyrimidin-4-yl)amino)hexanoic acid (992.0 mg, 100%) as a white solid. ^{1}H NMR (400 MHz, DMSO-d_6) δ 8.34 (d, *J* = 4.1 Hz, 1H), 7.77 (s, 1H), 7.61 (d, *J*

= 6.5 Hz, 1H), 7.53 (dd, *J* = 8.5, 4.2 Hz, 1H), 7.10 (m, 1H), 6.53 (d, *J* = 2.3 Hz, 1H), 6.42 (dd, *J* = 7.9, 2.0 Hz, 1H), 4.65 (m, 1H), 4.44 (m, 2H), 3.81 (s, 3H), 3.71 (s, 3H), 1.90 (m, 2H), 1.30 (m, 4H), 0.84 (m, 3H). LC/MS (*m*/*z*) 426.16 [M+1].

(*R*)-2-((2-((2,4-dimethoxybenzyl)amino)pyrido[3,2-*d*]pyrimidin-4-yl)amino)hexanoic acid (10.9 mg, 0.02 mmol) was treated with TFA (3 mL) and the mixture stirred for 2.5 h. The reaction was concentrated under reduced pressure and then the residue co-evaporated with MeOH (3 x 20 mL). The residue was suspended in MeOH and filtered. The solution was concentrated under reduced pressure to provide (*R*)-**6h** (17.3 mg, 100%) as a TFA salt. ^{1}H NMR (400 MHz, MeOH-d_4) δ 8.67 (dd, *J* = 4.4, 1.4 Hz, 1H), 7.89 (dd, *J* = 8.5, 1.5 Hz, 1H), 7.79 (dd, *J* = 8.5, 4.4 Hz, 1H), 4.97 (dd, *J* = 8.4, 5.0 Hz, 1H), 2.23 – 2.08 (m, 1H), 2.08 – 1.96 (m, 1H), 1.47 – 1.37 (m, 4H), 0.93 (t, *J* = 7.1 Hz, 3H). LC/MS (*m*/*z*) 276.12 [M+1].

(*R*)-2-((2-aminopyrido[3,2-*d*]pyrimidin-4-yl)amino)hexanamide ((*R*)-6i). (*R*)-2-((2-((2,4-dimethoxybenzyl)amino)pyrido[3,2-*d*]pyrimidin-4-yl)amino)hexanoic acid (50 mg, 0.12 mmol, see example (*R*)-**6h**) in NMP (6 mL) was treated with 0.5 M ammonia in 1,4-dioxane (1.2 mL, 0.6 mmol), *N*,*N*-diisopropylethylamine (1.2 mL, 6.89 mmol), and HATU (174.2 mg, 0.46 mmol). The mixture was stirred for 3.5 h, and then the mixture was subjected to reverse phase preparative HPLC (10%-70% CH_3CN in water with 0.1% TFA on a Synergi 4μ Polar-RP 80A Axia over a 20 min gradient) to provide (*R*)-2-((2-((2,4-dimethoxybenzyl)amino)pyrido[3,2-*d*]pyrimidin-4-yl)amino)hexanamide (7.4 mg, 14%). LC/MS (*m*/*z*) 425.13 [M+1].

(*R*)-2-((2-((2,4-dimethoxybenzyl)amino)pyrido[3,2-*d*]pyrimidin-4-yl)amino)hexanamide (7.4 mg, 0.02 mmol) was treated with TFA (3 mL) and the mixture stirred for 4.5 h. The reaction was concentrated under reduced pressure and co-evaporated with MeOH (3 x 20 mL). The residue was subjected to reverse phase preparative HPLC (10%-60% CH_3CN

in water with 0.1% TFA on a Synergi 4µ Polar-RP 80A Axia over a 20 min gradient) to provide (*R*)-**6i** (1.5 mg, 22%) as a TFA salt. ^{1}H NMR (400 MHz, MeOH-d_4) δ 8.69 (dd, *J* = 4.3, 1.5 Hz, 1H), 7.85 (dd, *J* = 8.5, 1.5 Hz, 1H), 7.80 (dd, *J* = 8.5, 4.3 Hz, 1H), 2.17 – 2.03 (m, 1H), 2.03 – 1.90 (m, 1H), 1.50 – 1.35 (m, 4H), 0.93 (t, *J* = 6.9 Hz, 3H). LC/MS (*m*/*z*) 275.17 [M+1].

(*R*)-2-((2-aminopyrido[3,2-*d*]pyrimidin-4-yl)amino)-*N*-methylhexanamide ((*R*)-6j). (*R*)-2-((2-((2,4-dimethoxybenzyl)amino)pyrido[3,2-*d*]pyrimidin-4-yl)amino)hexanoic acid (100 mg, 0.24 mmol, see example (*R*)-**6h**) in NMP (10 mL) was treated with 2 M methylamine in THF (0.25 mL, 0.5 mmol), *N*,*N*-diisopropylethylamine (0.20 mL, 1.17 mmol), and HATU (138 mg, 0.36 mmol). The mixture was stirred for 2.5 h and then subjected to reverse phase preparative HPLC (20%-60% CH_3CN in water with 0.1% TFA on a Synergi 4µ Polar-RP 80A Axia over a 20 min gradient) to provide (*R*)-2-((2-((2,4-dimethoxybenzyl)amino)pyrido[3,2-*d*]pyrimidin-4-yl)amino)-*N*-methylhexanamide (22.6 mg, 18%). LC/MS (*m*/*z*) 439.15 [M+1].

(*R*)-2-((2-((2,4-dimethoxybenzyl)amino)pyrido[3,2-*d*]pyrimidin-4-yl)amino)-*N*-methylhexanamide (22.6 mg, 0.05 mmol) was treated with TFA (3 mL) and the mixture stirred for 3.5 h. The reaction was concentrated under reduced pressure and then co-evaporated with MeOH (3 x 20 mL). The residue was subjected to reverse phase preparative HPLC (10%-60% CH_3CN in water with 0.1% TFA on a Synergi 4µ Polar-RP 80A Axia over a 20 min gradient) to provide (*R*)-**6j** (8.8 mg, 42%) as a TFA salt. ^{1}H NMR (400 MHz, MeOH-d_4) δ 8.68 (dd, *J* = 4.4, 1.5 Hz, 1H), 7.87 (dd, *J* = 8.5, 1.5 Hz, 1H), 7.80 (dd, *J* = 8.5, 4.3 Hz, 1H), 4.82 (dd, *J* = 8.3, 5.5 Hz, 1H), 2.77 (s, 3H), 2.14 – 2.00 (m, 1H), 2.00 – 1.86 (m, 1H), 1.52 – 1.32 (m, 4H), 0.94 (t, *J* = 7.0 Hz, 3H). LC/MS (*m*/*z*) 289.23 [M+1].

(*S*)-2-((2-amino-7-fluoropyrido[3,2-*d*]pyrimidin-4-yl)amino)-2-methylhexan-1-ol ((*S*)-7). Compound **32** (140 mg, 78 mmol) and (*S*)-**18c** (125 mg, 0.95 mmol) in NMP (7.5 mL),

were treated with 1,8-diazabicyclo[5.4.0]undec-7-ene (0.35 mL, 2.4 mmol) followed by (benzotriazol-1-yloxy)tris(dimethylamino)phosphonium hexafluorophosphate (419 mg, 0.95 mmol). The mixture was stirred for 16 h and then subjected to reverse phase preparative HPLC (10%-50% CH_3CN in water with 0.1% TFA on a Gemini 10µ C18 110A Axia over a 20 min gradient) to provide **(*S*)-7** (45 mg, 20%) as a TFA salt. ^{1}H NMR (400 MHz, MeOH-d_4) δ 8.55 (d, J = 2.4 Hz, 1H), 7.63 (dd, J = 8.7, 2.5 Hz, 1H), 3.97 (d, J = 11.2 Hz, 1H), 3.71 (d, J = 11.2 Hz, 1H), 2.15 – 2.04 (m, 1H), 1.98 – 1.87 (m, 1H), 1.54 (s, 3H), 1.41 – 1.31 (m, 4H), 0.92 (t, J = 6.9 Hz, 3H). ^{19}F NMR (377 MHz, MeOH-d_4) δ -118.22 (d, J = 8.7 Hz). LC/MS (*m/z*) 294.1 [M+1].

(*R*)-2-((2-amino-7-fluoropyrido[3,2-*d*]pyrimidin-4-yl)amino)-2-methylhexan-1-ol ((*R*)-7). Compound **25** (9.5 g, 43.6 mmol) and (*R*)-**18c** (5.5 g, 41.9 mmol) in 2-methyl THF (400 ml) was treated with *N*,*N*-diisopropylethylamine (29 mL, 167.7 mmol) and the mixture heated at reflux for 4 h. The reaction was cooled to rt, and solids removed by filtration. The eluant was concentrated under reduced pressure and the residue diluted in EtOAc (300 mL) and H_2O (300 mL). The organics were separated and then washed with brine (100 mL), dried over Na_2SO_4, filtered, and concentrated under reduced pressure to ~75 mL. To this concentrated solution, hexanes (200 mL) was slowly added via addition funnel with stirring to induce precipitation. The resulting solid product was filtered and air dried to provide (*R*)-2-((2-chloro-7-fluoropyrido[3,2-*d*]pyrimidin-4-yl)amino)-2-methylhexan-1-ol (7.7 g, 58.7%) as a tan solid. The mother liquor was subjected to silica gel chromatography eluting with 0-100% EtOAc-hexanes to provide additional product (3.3 g, 25.2%). ^{1}H NMR (400 MHz, $CHCl_3$-d_1) δ 8.56 (d, J = 2.6 Hz, 1H), 7.74 (dd, J = 8.8, 2.2 Hz, 1H), 7.50 (d, J = 13.5 Hz, 1H), 3.86 (d, J = 12.1 Hz, 1H), 3.81 (d, J = 12.1 Hz, 1H), 1.95 (ddd, J = 13.6, 11.8, 4.4 Hz, 1H), 1.82 (ddd, J = 13.7, 11.9, 4.2 Hz, 1H), 1.46 (s, 3H), 1.44 – 1.23 (m, 4H), 0.93 (t, J = 7.1 Hz, 3H). ^{19}F NMR (377 MHz, $CHCl_3$-d_1) δ -116.77.

LC/MS (*m/z*) 313.3 [M+1].

(*R*)-2-((2-chloro-7-fluoropyrido[3,2-d]pyrimidin-4-yl)amino)-2-methylhexan-1-ol (5.9 g, 18.9 mmol) in 2-methyl THF (200 mL) was treated with Dmb-NH_2 (7.0 mL, 46.6 mmol) and *N*,*N*-diisopropylethylamine (10.0 mL, 57.4 mmol). The reaction vessel was then sealed and heated at 110°C for 8 h. The mixture was then allowed to cool to rt, diluted with EtOAc (500 mL), washed with water (500 mL), brine (300 mL), dried over Na_2SO_4, filtered, and concentrated under reduced pressure. The residue was subjected to silica gel chromatography eluting with 0-100% EtOAc-hexanes, to provide (*R*)-2-((2-((2,4-dimethoxybenzyl)amino)-7-fluoropyrido[3,2-*d*]pyrimidin-4-yl)amino)-2-methylhexan-1-ol (7.02 g, 84%). ^{1}H NMR (400 MHz, $CHCl_3$-d_1) δ 8.13 (d, *J* = 2.5 Hz, 1H), 7.33 (s, 1H), 7.28 (s, 1H), 7.10 (s, 1H), 6.46 (d, *J* = 2.4 Hz, 1H), 6.42 (dd, *J* = 8.2, 2.4 Hz, 1H), 4.56 (d, *J* = 5.8 Hz, 2H), 3.84 (s, 3H), 3.79 (s, 3H), 3.76 (s, 2H), 1.91 (m, 1H), 1.74 (m, 2H), 1.39 (s, 3H), 1.48 – 1.28 (m, 4H), 0.91 (t, *J* = 7.0 Hz, 4H). ^{19}F NMR (377 MHz, $CHCl_3$-d_1) δ -121.34. LC/MS (*m/z*) 444.2 [M+1].

(*R*)-2-((2-((2,4-dimethoxybenzyl)amino)-7-fluoropyrido[3,2-*d*]pyrimidin-4-yl)amino)-2-methylhexan-1-ol (9.5 g, 21.4 mmol) was dissolved in TFA (200 mL) and the mixture stirred for 3 h. The mixture was concentrated under reduced pressure and the residue was diluted with MeOH (80 mL) and the mixture stirred for 16 h. The mixture was filtered and the solids rinsed with MeOH (3 x 20 mL). The eluant was concentrated under reduced pressure and the residue co-evaporated with toluene and dried under vacuum. The solid was then dissolved in Et_2O (300 mL), washed with sat. $NaHCO_3$ solution (3 x 100 mL), brine (100 mL), dried over Na_2SO_4, and concentrated under reduced pressure to provide (*R*)-**7** (5.5 g, 88%). ^{1}H NMR (400 MHz, MeOH-d_4) δ 8.25 (d, *J* = 2.6 Hz, 1H), 7.26 (dd, *J* = 10.1, 2.6 Hz, 1H), 3.92 (d, *J* = 11.3 Hz, 1H), 3.73 (d, *J* = 11.3 Hz, 1H), 2.16 – 2.03 (m, 1H), 1.87 – 1.76 (m, 1H), 1.46 (s, 3H), 1.43 – 1.26 (m, 4H),

0.91 (t, J = 7.0 Hz, 3H). ^{19}F NMR (377 MHz, MeOH-d_4) δ -123.39 (d, J = 10.0 Hz). LC/MS (*m/z*) 294.1 [M+1].

4-butoxypyrido[3,2-*d*]pyrimidin-2-amine (10). Compound **8** (50 mg, 0.25 mmol, CAS# 39551-54-7, Astatech, Inc., Bristol, PA) in THF (2 mL) was treated with butan-1-ol (0.03 mL, 0.28 mmol) and NaH 60% oil dispersion (12 mg, 0.3 mmol). The reaction mixture was stirred for 6 h and then diluted with EtOAc (50 mL), washed with water (50 mL), brine (50 mL), dried over Na_2SO_4, and concentrated under reduced pressure. The residue was subjected to silica gel chromatography eluting with 0-100% EtOAc-hexanes to provide 4-butoxy-2-chloropyrido[3,2-*d*]pyrimidine (42 mg, 71%). LC/MS (*m/z*) 237.91 [M+1]. The 4-butoxy-2-chloropyrido[3,2-*d*]pyrimidine (42 mg, 0.18mmol) in THF (10 mL) was then treated with Dmb-NH_2 (0.19 ml, 1.25 mmol) and *N*,*N*-diisopropylethylamine (0.13 ml, 0.75 mmol) and the mixture heated at 100°C for 16 h. The reaction was cooled to rt, diluted with EtOAc (20 mL), washed with water (20 mL), brine (20 mL), dried over Na_2SO_4, and concentrated under reduced pressure. The residue was subjected to silica gel chromatography eluting with 0-40% EtOAc-hexanes to provide **9** (24 mg, 37%). LC/MS (*m/z*) 369.07 [M+1].

Compound **9** (24 mg, 0.07 mmol) was treated with TFA (3 mL) and the mixture stirred for 1 h. The mixture was diluted with water and MeOH and stirred for 1 h before concentration under reduced pressure. The residue was co-evaporated with MeOH (3 x 20 mL), suspended in MeOH, and filtered. The eluant was concentrated under reduced pressure and the residue subjected to reverse phase preparative HPLC (10%-70% CH_3CN in water with 0.1% TFA on a Synergi 4μ Polar-RP 80A Axia over a 20 min gradient) to provide **10** (2 mg, 9%) as a TFA salt. ^{1}H NMR (400 MHz, MeOH-d_4) δ 8.75 (dd, J = 4.4, 1.4 Hz, 1H), 7.99 (dd, J = 8.6, 1.4 Hz, 1H),

7.89 (dd, *J* = 8.6, 4.3 Hz, 1H), 4.73 (t, *J* = 6.6 Hz, 2H), 1.99 – 1.89 (m, 2H), 1.62 – 1.52 (m, 2H), 1.03 (t, *J* = 7.4 Hz, 3H). LC/MS (*m/z*) 218.95 [M+1].

(*R*)-2-((2-aminoquinazolin-4-yl)amino)hexan-1-ol ((*R*)-14). Compound **13** (20 mg, 0.12 mmol) and (benzotriazol-1-yloxy)tris(dimethylamino)phosphonium hexafluorophosphate (66.0 mg, 0.15 mmol) were suspended in DMF (1.3 mL) and treated with 1,8-diazabicyclo[5.4.0]undec-7-ene (0.05 mL, 0.27 mmol). The mixture was stirred for 4.5 h, (*R*)-**11d** (39 mg, 0.27 mmol) was added, and after 16 h, the reaction mixture was subjected to reverse phase preparative HPLC (10%-70% CH_3CN in water with 0.1% TFA on a Synergi 4µ Polar-RP 80A Axia over a 20 min gradient) to provide (*R*)-**14** (33.2 mg, 71%) as a TFA salt. ^{1}H NMR (400 MHz, MeOH-d_4) δ 8.23 – 8.21 (m, 1H), 7.80 – 7.76 (m, 1H), 7.50 – 7.33 (m, 2H), 4.71 – 4.56 (m, 1H), 3.80 – 3.61 (m, 2H), 1.81 – 1.64 (m, 2H), 1.47 – 1.31 (m, 4H), 0.92 (m, 3H). LC/MS (*m/z*) 261.1 [M+1].

***(S)*-2-((2-aminoquinazolin-4-yl)amino)hexan-1-ol ((*S*)-14).** The same procedure as (*R*)-**14,** except with addition of (*S*)-**11d,** provided (*S*)-**14** (29 mg, 62 %) as a TFA salt. ^{1}H NMR (400 MHz, MeOH-d_4) δ 8.23 – 8.21 (m, 1H), 7.80 – 7.76 (m, 1H), 7.45 – 7.39 (m, 2H), 4.71 – 4.56 (m, 1H), 3.80 – 3.61 (m, 2H), 1.81 – 1.64 (m, 2H), 1.47 – 1.31 (m, 4H), 0.92 (m, 3H). LC/MS (*m/z*) 261.1 [M+1].

(*R*)-2-((2-aminoquinolin-4-yl)amino)hexan-1-ol ((*R*)-16). Compound **15** (50 mg, 0.28 mmol), (*R*)-**11d** (82.01 mg, 0.7 mmol), bis(dibenzylideneacetone)palladium(0) (8.08 mg, 0.01 mmol) , sodium tert-butoxide (53.8 mg, 0.56 mmol) and (*R*)-(+)-2,2'-bis(diphenylphosphino)-1,1'-binaphthyl (9.11 mg, 0.01 mmol) were added to 1,4-dioxane (4 mL) and the mixture heated in a sealed vial at 135°C for 4 h. The reaction was then diluted with minimal water and MeOH, filtered and then subjected to reverse phase preparative HPLC (5%-50% CH_3CN in water with

0.1% TFA on a Synergi 4μ Polar-RP 80A Axia over a 20 min gradient) to provide (*R*)-**16** (12 mg, 16 %) as a TFA salt. ^{1}H NMR (400 MHz, MeOH-d_4) δ 8.30 – 8.27 (m, 1H), 7.83 – 7.79 (m, 1H), 7.63 – 7.60 (m, 1H), 7.54 – 7.50 (m, 1H), 6.48 (s, 1H), 4.57 (dd, *J* = 10.8, 3.2 Hz, 1H), 4.45 (dd, *J* = 10.7, 6.1 Hz, 1H), 3.84 – 3.78 (m, 1H), 1.93 – 1.86 (m, 2H), 1.62 – 1.35 (m, 4H), 0.99 (t, *J* = 7.0 Hz, 3H). LC/MS (*m/z*) 260.0 [M+1].

(*S*)-2-((2-aminoquinolin-4-yl)amino)hexan-1-ol ((*S*)-16). The same procedure as (*R*)-**16,** except with the addition of (*S*)-**11d** (82.01 mg, 0.7 mmol)**,** provided (*S*)-**16** (5.1 mg, 7 %) as a TFA salt. ^{1}H (400 MHz, MeOH-d_4) δ 8.30 – 8.28 (m, 1H), 7.83 – 7.79 (m, 1H), 7.66 – 7.58 (m, 1H), 7.54 – 7.50 (m, 1H), 6.47 (s, 1H), 4.57 (dd, *J* = 10.8, 3.2 Hz, 1H), 4.45 (dd, *J* = 10.7, 6.1 Hz, 1H), 3.84 – 3.79 (m, 1H), 1.95 – 1.84 (m, 2H), 1.62 – 1.35 (m, 4H), 0.99 (t, *J* = 7.0 Hz, 3H). LC/MS (*m/z*) 260.0 [M+1].

(*R*)-2-((2-aminopyrido[3,2-*d*]pyrimidin-4-yl)amino)-2-methylpentan-1-ol ((*R*)-23a). Compound **8** (540 mg, 2.71 mmol) was treated with dioxane (15 mL) followed by *N,N*-diisopropylethylamine (1.9 mL, 10.8 mmol), and (*R*)-**18a** (486 mg, 2.71 mmol). The reaction mixture was stirred at 80°C for 15 min, then additional **8** (250 mg, 1.25 mmol) was added. The mixture was stirred at 80°C overnight then treated with Dmb-NH_2 (0.80 mL, 5.0 mmol) and the mixture heated at 120℃ overnight. The reaction mixture was partitioned between EtOAc (50 mL) and H_2O (50 mL), the organic layer separated, dried over $MgSO_4$, and concentrated under reduced pressure. The residue was subjected to silica gel chromatography eluting with 0-100% EtOAc-hexanes to provide methyl (*R*)-2-((2-((2,4-dimethoxybenzyl)amino)pyrido[3,2-*d*]pyrimidin-4-yl)amino)-2-methylpent-4-enoate (634 mg, 54%). LC/MS (*m/z*) 438.2 [M+1].

Methyl (*R*)-2-((2-((2,4-dimethoxybenzyl)amino)pyrido[3,2-*d*]pyrimidin-4-yl)amino)-2-methylpent-4-enoate (634 mg, 1.44 mmol) was treated with THF (20 mL) and 1M lithium

aluminum hydride in Et_2O (3.6 mL, 3.6 mmol). The reaction mixture was stirred for 2 h and then quenched with water (100 mL) and extracted with EtOAc (100 mL). The organic layer was separated, dried over $MgSO_4$, and concentrated under reduced pressure. The residue was subjected to silica gel chromatography eluting with 0-100% EtOAc-hexanes to provide (*R*)-**22a** (168 mg, 28%). LC/MS (*m/z*) 410.2 [M+1].

(*R*)-**22a** (35 mg, 0.09 mmol) was treated with Pd/C (60 mg) and EtOH (5 mL) and then stirred under H_2 for 24 h. The mixture was filtered and the eluant concentrated under reduced pressure. The residue was treated with CH_2Cl_2 (2 mL) and TFA (0.5 mL) and the mixture stirred for 3 h. The reaction mixture was concentrated under reduced pressure and subjected to reverse phase preparative HPLC (10-70% CH_3CN in water with 0.1% TFA using a Hydro-RP column) to provide (*R*)-**23a** (9.7 mg, 45%) as a TFA salt. ^{1}H NMR (400 MHz, DMSO-d_6) δ 7.85 – 7.61 (m, 2H), 7.42 – 7.25 (m, 3H), 6.05 (s, 1H), 3.65 (d, J = 8.6 Hz, 1H), 3.55 (d, J = 8.6 Hz, 1H), 1.71 – 1.41 (m, 4H), 1.45 (s, 3H), 0.90 – 0.75 (m, 3H). LC/MS (*m/z*) 262.1 [M+1].

2-((2-aminopyrido[3,2-*d*]pyrimidin-4-yl)amino)-2-butylhexan-1-ol (23b). Compound **18b** (109 mg, 0.42 mmol) in THF (10 mL) was treated with **8** (94 mg, 0.47 mmol) and *N,N*-diisopropylethylamine (0.15 mL, 0.76 mmol) and the mixture heated at 80°C for 20 h. Dmb-NH_2 (0.25 mL, 1.66 mmol) was added and the mixture was heated at 100°C for 24 h. The reaction mixture was cooled to rt, diluted with EtOAc (50 mL), washed with water (50 mL), brine (50 mL), dried over Na_2SO_4, and concentrated under reduced pressure. The residue was subjected to silica gel chromatography eluting with 0-100% EtOAc-hexanes to provide methyl 2-butyl-2-((2-((2,4-dimethoxybenzyl)amino)pyrido[3,2-*d*]pyrimidin-4-yl)amino)hexanoate (64.4 mg, 52%). LC/MS (*m*/*z*) 496.27 [M+1].

Methyl 2-butyl-2-((2-((2,4-dimethoxybenzyl)amino)pyrido[3,2-*d*]pyrimidin-4-yl)amino)hexanoate (64.4 mg) in THF (10 mL) at 0°C was treated with 1 M lithium aluminum hydride in Et_2O (0.9 mL, 0.9 mmol) and the mixture stirred for 3 h and allowed to warm to rt. The reaction was quenched with water (1 mL) followed by 2 M aq. NaOH (0.1 mL) and the slurry that formed was filtered, rinsed with EtOAc, and the filtrate concentrated under reduced pressure. The residue was subjected to silica gel chromatography eluting with 20-100% EtOAc-hexanes to provide 2-butyl-2-((2-((2,4-dimethoxybenzyl)amino)pyrido[3,2-*d*]pyrimidin-4-yl)amino)hexan-1-ol **22b** (21.1 mg, 35%). ^{1}H NMR (400 MHz, $CHCl_3$-d_1) δ 8.26 (dd, J = 4.2, 1.5 Hz, 1H), 7.67 (d, J = 8.3 Hz, 1H), 7.41 (dd, J = 8.5, 4.2 Hz, 1H), 7.35 – 7.17 (m, 2H), 6.46 (d, J = 2.4 Hz, 1H), 6.41 (dd, J = 8.2, 2.4 Hz, 1H), 4.55 (d, J = 5.7 Hz, 2H), 3.83 (s, 3H), 3.80 (s, 2H), 3.78 (s, 3H), 1.79 (tt, J = 13.6, 9.9 Hz, 4H), 1.45 – 1.19 (m, 8H), 0.91 (t, J = 7.0 Hz, 6H). LC/MS (*m*/*z*) 468.22 [M+1].

22b (21.1 mg, 0.05 mmol) was treated with TFA (3 mL) and the mixture stirred for 1 h. The reaction mixture was diluted with MeOH (10 mL), stirred for 1 h, and then concentrated under reduced pressure. The residue was co-evaporated with MeOH (3 x 20 mL), re-suspended in MeOH and filtered. The filtrate was concentrated under reduced pressure to provide **23b** (21.3 mg, 100%) as a TFA salt. ^{1}H NMR (400 MHz, MeOH-d_4) δ 8.61 (dd, J = 4.4, 1.4 Hz, 1H), 7.85 (dd, J = 8.5, 1.4 Hz, 1H), 7.76 (dd, J = 8.5, 4.4 Hz, 1H), 3.90 (s, 2H), 2.03 – 1.95 (m, 4H), 1.39 – 1.31 (m, 8H), 0.92 (t, J = 6.9 Hz, 6H). LC/MS (*m*/*z*) 318.15 [M+1].

(*R*)-2-((2-aminopyrido[3,2-*d*]pyrimidin-4-yl)amino)-2-methylhexan-1-ol (**(*R*)-23c**). Compound **8** (50 mg, 0.25 mmol) in THF (10 mL) was treated with (*R*)-**18c** (50 mg, 0.38 mmol) and *N,N*-diisopropylethylamine (0.13 mL, 0.75 mmol). The mixture was stirred at 80°C for 18 h, and then Dmb-NH_2 (0.19 mL, 1.25 mmol) was added. The mixture was heated at 100°C for 18 h,

cooled to rt, diluted with EtOAc, washed with water, brine, dried over Na_2SO_4, then filtered and concentrated under reduced pressure. The residue was subjected to silica gel chromatography eluting with 0-100% EtOAc-hexanes to provide (*R*)-2-((2-((2,4-dimethoxybenzyl)amino)pyrido[3,2-*d*]pyrimidin-4-yl)amino)-2-methylhexan-1-ol (18 mg, 17%). LC/MS (*m/z*) 426.2 [M+1]. The (*R*)-2-((2-((2,4-dimethoxybenzyl)amino)pyrido[3,2-*d*]pyrimidin-4-yl)amino)-2-methylhexan-1-ol (18 mg) was treated with TFA (3 mL) and the mixture stirred for 2 h. The reaction mixture was concentrated under reduced pressure and the residue subjected to reverse phase preparative HPLC (10%-70% CH_3CN in water with 0.1% TFA on a Synergi 4μ Polar-RP 80A Axia over a 20 min gradient) to provide (*R*)-**23c** (10 mg, 60%) as a TFA salt. ^{1}H NMR (400 MHz, MeOH-d_4) δ 8.63 (dd, *J* = 4.2, 1.6 Hz, 1H), 7.82 (dd, *J* = 8.5, 1.6 Hz, 1H), 7.78 (dd, *J* = 8.5, 4.2 Hz, 1H), 3.98 (d, *J* = 11.2 Hz, 1H), 3.73 (d, *J* = 11.2 Hz, 1H), 2.16 – 2.03 (m, 1H), 2.01 – 1.85 (m, 1H), 1.55 (s, 3H), 1.42 – 1.32 (m, 4H), 0.93 (t, *J* = 6.8 Hz, 3H). LC/MS (*m/z*) 276.1 [M+1].

(*S*)-2-((2-aminopyrido[3,2-*d*]pyrimidin-4-yl)amino)-2-methylhexan-1-ol ((*S*)-23c). The same procedure as (*R*)-**23c** (50 mg), except with the addition of (*S*)-**18c** (250 mg, 1.38 mmol, Astatech, Inc., Bristol, PA), provided (*S*)-**23c** (25 mg, 26% overall yield) as a TFA salt. ^{1}H NMR (400 MHz, MeOH-d_4) δ 8.61 (dd, *J* = 4.4, 1.4 Hz, 1H), 7.85 (dd, *J* = 8.5, 1.4 Hz, 1H), 7.76 (dd, *J* = 8.5, 4.4 Hz, 1H), 3.98 (d, *J* = 11.3 Hz, 1H), 3.73 (d, *J* = 11.3 Hz, 1H), 2.17 – 2.05 (m, 1H), 1.98 – 1.85 (m, 1H), 1.55 (s, 3H), 1.40 – 1.32 (m, 4H), 0.92 (t, *J* = 6.9 Hz, 3H). LC/MS (*m/z*) 276.1 [M+1].

(*R*)-2-((2-amino-7-fluoropyrido[3,2-*d*]pyrimidin-4-yl)amino)-2-methylheptan-1-ol ((*R*)-23d). The same procedure as (*R*)-**23c** (50 mg), except with the addition of (*R*)-**18d** (135 mg, 0.74 mmol), provided (*R*)-**23d** (9.3 mg, 7%) as a TFA salt. ^{1}H NMR (400 MHz, MeOH-d_4) δ

8.63 (dd, *J* = 4.3, 1.5 Hz, 1H), 7.86 – 7.80 (m, 1H), 7.77 (dd, *J* = 8.5, 4.3 Hz, 1H), 3.98 (d, *J* = 11.2 Hz, 1H), 3.72 (d, *J* = 11.2 Hz, 1H), 2.16 – 2.04 (m, 1H), 1.92 (tt, *J* = 11.1, 4.9 Hz, 1H), 1.55 (s, 3H), 1.42 – 1.28 (m, 6H), 0.93 – 0.85 (m, 3H). LC/MS (*m/z*) 290.2 [M+1].

(*R*)-2-((2-aminopyrido[3,2-*d*]pyrimidin-4-yl)amino)-2-methyloctan-1-ol ((*R*)-23e). (*R*)-**18e** (75 mg, 0.38 mmol) and **8** (76 mg, 0.38 mmol) in THF (2.5 mL) were treated with *N,N*-diisopropylethylamine (0.2 mL, 1.15 mmol) and the mixture stirred at 80°C for 24 h. The reaction was cooled to ambient temperature, diluted with EtOAc (25 mL), washed with water (25 mL) and brine (25 mL), dried over Na_2SO_4, then filtered and concentrated under reduced pressure. The residue was subjected to silica gel chromatography eluting with 0-50% EtOAc-hexanes to provide (*R*)-2-((2-chloropyrido[3,2-*d*]pyrimidin-4-yl)amino)-2-methyloctan-1-ol (85.6 mg, 69%). LC/MS (*m*/*z*) 323.11 [M+1].

(*R*)-2-((2-chloropyrido[3,2-*d*]pyrimidin-4-yl)amino)-2-methyloctan-1-ol (86 mg, 0.27 mmol) in 2-MeTHF (3.0 mL) was treated with K_2CO_3 (77 mg, 0.55 mmol) followed by Dmb-NH_2 (0.09 mL, 0.55 mmol) and the mixture stirred at 85°C for 18 h. The reaction was cooled to ambient temperature, diluted with EtOAc (25 mL), washed with water (20 mL) and brine (20 mL), dried over Na_2SO_4, then filtered and concentrated under reduced pressure. The residue was subjected to silica gel chromatography eluting with 20-100% EtOAc-hexanes to provide (*R*)-2-((2-((2,4-dimethoxybenzyl)amino)pyrido[3,2-*d*]pyrimidin-4-yl)amino)-2-methyloctan-1-ol (64.6 mg, 54%). ^{1}H NMR (400 MHz, $CHCl_3$-d_1) δ 8.27 (dd, *J* = 4.2, 1.4 Hz, 1H), 7.69 (d, *J* = 8.4 Hz, 1H), 7.42 (dd, *J* = 8.4, 4.2 Hz, 1H), 7.29 (d, *J* = 8.2 Hz, 1H), 7.24 (s, 1H), 6.46 (d, *J* = 2.3 Hz, 1H), 6.42 (dd, *J* = 8.2, 2.4 Hz, 1H), 4.57 (d, *J* = 5.8 Hz, 2H), 3.84 (s, 3H), 3.79 (s, 3H), 3.76 (s, 2H), 2.00 – 1.90 (m, 1H), 1.79 – 1.68 (m, 1H), 1.39 (s, 3H), 1.31 – 1.26 (m, 8H), 0.87 (t, *J* = 7.7 Hz, 3H). LC/MS (*m*/*z*) 454.20 [M+1].

(*R*)-2-((2-((2,4-dimethoxybenzyl)amino)pyrido[3,2-*d*]pyrimidin-4-yl)amino)-2-methyloctan-1-ol (57 mg, 0.13 mmol) was treated with TFA (3 mL), the mixture stirred for 3.5 h, and then concentrated under reduced pressure. The residue was co-evaporated with MeOH (3 x 20 mL), then suspended in MeOH and filtered. The filtrate was stirred for 16 h, and then concentrated under reduced pressure to provide (*R*)-**23e** (48 mg, 91%) as a TFA salt. ^{1}H NMR (400 MHz, MeOH-d_4) δ 8.60 (dd, J = 4.4, 1.4 Hz, 1H), 7.85 (dd, J = 8.5, 1.4 Hz, 1H), 7.76 (dd, J = 8.5, 4.4 Hz, 1H), 3.98 (d, J = 11.2 Hz, 1H), 3.73 (d, J = 11.3 Hz, 1H), 2.15 – 2.04 (m, 1H), 1.97 – 1.86 (m, 1H), 1.54 (s, 3H), 1.36 – 1.27 (m, 8H), 0.87 (t, J = 6.6 Hz, 3H). LC/MS (*m*/*z*) 304.15 [M+1].

2,4-dichloro-7-fluoropyrido[3,2-*d*]pyrimidine (25). 3-Amino-2-bromo-5-fluoropyridine **24** (25 g, 131 mmol, Astatech, Inc., Bristol, PA) was treated with $ZnCN_2$ (16.9 g, 144 mmol), $Pd(Ph_3)_4$ (11.3 g, 9.8 mmol) in DMF (200 mL) and heated at 115°C . The mixture was stirred for 6 h and then allowed to cool and concentrated under reduced pressure to a solid. The solid was washed with EtOAc (2 x) and filtered. The organic layers were combined, washed water (3 x), sat. aq. NH_4Cl, dried over $MgSO_4$, filtered and concentrated under reduced pressure to provide crude 3-amino-5-fluoropicolinonitrile (19.8 g, quant.). ^{1}H NMR (400 MHz, DMSO-d_6) δ 7.86 (d, J = 2.4 Hz, 1H), 7.01 (dd, J = 11.0, 2.5 Hz, 1H), 6.55 (s, 2H). ^{19}F NMR (377 MHz, DMSO-d_6) δ -119.65 (d, J = 11.0 Hz).

The crude 3-amino-5-fluoropicolinonitrile (2.6 g, 19.0 mmol) in DMSO (10 mL) was cooled to 0°C, treated with K_2CO_3 (524 mg, 3.8 mmol) followed by slow addition of H_2O_2 (2.3 mL, 22.8 mmol, 30% water). The cooling bath was removed and the reaction mixture stirred for 1 h. The reaction mixture was diluted with water (100 mL), extracted with EtOAc (3 x 100) and the combined organic layers washed with water (3 x 500), sat. aq. NH_4Cl (500 mL), dried over

$MgSO_4$, filtered and concentrated under reduced pressure. The crude residue of 3-amino-5-fluoropicolinamide (2.59 g, 85%) was used without further purification. LC/MS (*m/z*) 155.9 [M+1].

Crude 3-amino-5-fluoropicolinamide (1 g, 6.4 mmol) in dioxane (20 mL) was treated with triphosgene (1.9 g, 6.4 mmol) and the mixture heated to 110°C for 30 min. The reaction mixture was allowed to cool, concentrated under reduced pressure, and the residue washed with CH_2Cl_2, Et_2O, and air dried to provide 7-fluoropyrido[3,2-*d*]pyrimidine-2,4-diol (1.03 g, 90%). LC/MS (*m/z*) 182.0 [M+1].

7-Fluoropyrido[3,2-*d*]pyrimidine-2,4-diol (13.7 g, 75.6 mmol) was treated with phosphorus pentachloride (63.0 g, 302.6 mmol) and phosphorus (V) oxychloride (63g, 303 mmol, 4 equiv.) and heated to 110°C under a under reflux condenser for 8 h. The reaction mixture was concentrated under reduced pressure and azeotroped with toluene. The resultant solid was treated with EtOAc (500 mL) and ice-water (500 mL). The organic layer was separated and washed with saturated $NaHCO_3$ solution (500 mL), water (500 mL), sat. aq. NH_4Cl (500 mL), dried over $MgSO_4$, filtered and concentrated under reduced pressure to provide **25** (12.3 g, 75%). ^{1}H NMR (400 MHz, $CHCl_3$-d_1) δ 9.01 (d, J = 2.6 Hz, 1H), 7.94 (dd, J = 7.9, 2.7 Hz, 1H). ^{19}F NMR (377 MHz, $CHCl_3$-d_1) δ -111.79 (d, J = 7.9 Hz). LC/MS (*m/z*) 213.9 $[M+1+(OMe)-Cl]^+$.

(*R*)-2-((2-amino-7-fluoropyrido[3,2-*d*]pyrimidin-4-yl)amino)-2-methylhexane-1,6-diol ((*R*)-26a). Compound **25** (289 mg, 1.32 mmol) and (*R*)-**18f** (240 mg, 1.32 mmol) in 2,4-dioxane (13 mL) was treated with *N,N*-diisopropylethylamine (0.7 mL, 3.96 mmol) and the mixture stirred at 80°C for 4 h. The reaction mixture was cooled, diluted with EtOAc (500 mL), washed with brine (400 mL), dried over Na_2SO_4, then filtered and concentrated under reduced

pressure to provide (*R*)-2-((2-chloro-7-fluoropyrido[3,2-*d*]pyrimidin-4-yl)amino)-2-methylhexane-1,6-diol that was used without further purification. LC/MS (*m*/*z*) 329.07 [M+1]. The residue in 2-MeTHF (8.5 mL) was treated with K_2CO_3 (369 mg, 2.64 mmol) followed by Dmb-NH_2 (0.4 mL, 2.64 mmol) and stirred at 85°C for 18 h. The reaction mixture was cooled, filtered, concentrated under reduced pressure, and the residue subjected to silica gel chromatography eluting with 20-100% EtOAc-hexanes to provide (*R*)-2-((2-((2,4-dimethoxybenzyl)amino)-7-fluoropyrido[3,2-*d*]pyrimidin-4-yl)amino)-2-methylhexane-1,6-diol (410 mg, 66% over two steps). ^{1}H NMR (400 MHz, $CHCl_3$- d_1) δ 8.14 (s, 1H), 7.35 (d, *J* = 8.9 Hz, 1H), 7.27 (s, 1H), 6.47 (d, *J* = 2.3 Hz, 1H), 6.42 (dd, *J* = 8.2, 2.4 Hz, 1H), 4.57 (d, *J* = 5.8 Hz, 2H), 3.85 (s, 3H), 3.79 (s, 3H), 3.79 – 3.73 (m, 2H), 3.65 (t, *J* = 5.9 Hz, 2H), 2.03 – 1.89 (m, 1H), 1.89 – 1.78 (m, 1H), 1.65 – 1.47 (m, 4H), 1.47 – 1.33 (m, 3H). LC/MS (*m*/*z*) 460.22 [M+1].

(*R*)-2-((2-((2,4-dimethoxybenzyl)amino)-7-fluoropyrido[3,2-*d*]pyrimidin-4-yl)amino)-2-methylhexane-1,6-diol (53 mg, 0.12 mmol) was treated with TFA (3 mL) and the mixture stirred for 1 h. The reaction mixture was concentrated under reduced pressure and co-evaporated with MeOH (3 x 20 mL). The residue was suspended in MeOH, filtered and stirred overnight. The mixture was subjected to reverse phase preparative HPLC (Synergi 4u Polar-RP 80A, Axia; 20% aq. CH_3CN – 50% aq. CH_3CN, over 20 min gradient) to provide (*R*)-**26a** (19.8 mg, 55%) as a white solid. ^{1}H NMR (400 MHz, MeOH-d_4) δ 8.23 (d, *J* = 2.3 Hz, 1H), 7.25 (dd, *J* = 10.2, 2.5 Hz, 1H), 3.94 (d, *J* = 11.2 Hz, 1H), 3.73 (d, *J* = 11.3 Hz, 1H), 3.54 (t, *J* = 6.4 Hz, 2H), 2.17 – 2.07 (m, 1H), 1.90 – 1.80 (m, 1H), 1.55 (p, *J* = 6.9 Hz, 2H), 1.47 (s, 3H), 1.45 – 1.24 (m, 2H). ^{19}F NMR (377 MHz, MeOH-d_4) δ -123.39 (d, *J* = 10.2 Hz). LC/MS (*m*/*z*) 310.14 [M+1].

(*R*)-2-((2-amino-7-fluoropyrido[3,2-*d*]pyrimidin-4-yl)amino)-2-methylhexanoic acid ((*R*)-26b). Compound **25** (200 mg, 0.92 mmol) in THF (10 mL) was treated with (*R*)-**18g**

(250 mg, 1.4 mmol) and *N,N*-diisopropylethylamine (1.3 mL, 7.50 mmol) and the mixture heated at 80°C for 4 h. Dmb-NH_2 (1.9 mL, 12.5 mmol), *N,N*-diisopropylethylamine (1.3 mL, 7.50 mmol), and THF (5 mL) were then added and the mixture was heated at 110°C for 16 h. The reaction mixture was analysed by LC/MS to confirm amine addition and loss of the ester group. The reaction mixture was cooled, diluted with EtOAc (50 mL), washed with water (50 mL), brine (50 mL), dried over Na_2SO_4, and concentrated under reduced pressure to provide (*R*)-2-((2-((2,4-dimethoxybenzyl)amino)-7-fluoropyrido[3,2-*d*]pyrimidin-4-yl)amino)-2-methylhexanoic acid (300 mg, 66%). LC/MS (*m/z*) 458.19 [M+1]. (*R*)-2-((2-((2,4-dimethoxybenzyl)amino)-7-fluoropyrido[3,2-*d*]pyrimidin-4-yl)amino)-2-methylhexanoic acid was treated with TFA (3 mL) and the mixture stirred for 2.5 h. The reaction mixture was concentrated under reduced pressure and co-evaporated with MeOH (3 x 20 mL). The residue was suspended in MeOH, filtered, and the eluant concentrated under reduced pressure to provide (*R*)-**26b** (8 mg, 29%) as a TFA salt. ^{1}H NMR (400 MHz, MeOH-d_4) δ 9.10 (s, 1H), 8.59 (d, *J* = 2.4 Hz, 1H), 7.64 (dd, *J* = 8.7, 2.5 Hz, 1H), 3.98 – 3.84 (m, 2H), 3.85 – 3.63 (m, 2H), 2.61 (ddd, *J* = 13.6, 11.6, 4.9 Hz, 1H), 2.06 (ddd, *J* = 13.7, 11.3, 5.1 Hz, 1H), 1.81 (s, 3H), 1.44 – 1.07 (m, 5H), 0.88 (t, *J* = 7.2 Hz, 3H). LC/MS (*m/z*) 308.17 [M+1].

(2*R*,3*R*,4*R*,5*S*,6*R*)-6-(((*R*)-2-((2-amino-7-fluoropyrido[3,2-*d*]pyrimidin-4-yl)amino)-2-methylhexanoyl)oxy)-3,4,5-trihydroxytetrahydro-2*H*-pyran-2-carboxylic acid ((*R*)-26c). Produced by Hypha Discovery, Uxbridge, United Kingdom, using microbial (actinomycete) fermentation of (*R*)-**7** followed by reverse phase preparative HPLC purification to provide the glucuronide (*R*)-**26c**. ^{1}H NMR (499 MHz, CH_3CN-d_3) δ 7.71 (dd, *J* = 5.1, 2.6 Hz, 1H), 7.60 (s, 1H), 6.78 (dd, *J* = 10.6, 2.6 Hz, 1H), 6.46 (d, *J* = 11.4 Hz, 1H), 5.93 (s, 2H), 4.56 – 4.29 (m, 2H), 3.65 (ddd, *J* = 44.0, 28.8, 8.8 Hz, 2H), 3.09 (dd, *J* = 16.3, 9.9 Hz, 1H), 2.56 (d, *J* = 9.0 Hz, 1H),

2.43 (d, J = 9.5 Hz, 1H), 1.59 – 1.42 (m, 1H), 1.37 (t, J = 12.5 Hz, 1H), 0.92 (d, J = 6.9 Hz, 2H), 0.70 (dd, J = 14.3, 8.6 Hz, 3H), 0.45 (d, J = 7.7 Hz, 1H), 0.29 (td, J = 7.0, 4.2 Hz, 2H). LC/MS (*m/z*) 470.0 [M+1].

(*R*)-2-((7-chloro-2-((2,4-dimethoxybenzyl)amino)pyrido[3,2-*d*]pyrimidin-4-yl)amino)-2-methylhexan-1-ol (28). Compound **27**[29] (50 mg, 0.21 mmol) and (*R*)-**18c** (45 mg, 0.45 mmol) in THF (5 mL) was treated with *N,N*-diisopropylethylamine (0.16 mL, 0.90 mmol) and the mixture was then heated at 80°C for 24 h. The reaction was cooled, diluted with EtOAc (50 mL), washed with water (50 mL), brine (50 mL), dried over Na_2SO_4, and concentrated under reduced pressure. The residue was subjected to silica gel chromatography eluting with 0-100% EtOAc-hexanes to provide a yellow solid. The yellow solid was dissolved in THF (5 mL) and treated with Dmb-NH_2 (0.25 mL, 1.51 mmol) and *N,N*-diisopropylethylamine (0.16 mL, 0.90 mmol) and the mixture heated at 100°C for 16 h. The reaction was cooled, diluted with EtOAc (100 mL), washed with water (100 mL), brine (100 mL), dried over Na_2SO_4, and concentrated under reduced pressure. The residue was subjected to silica gel chromatography eluting with 20-100% EtOAc-hexanes to provide **28** (71.1 mg, 52% over 2 steps). ^{1}H NMR (400 MHz, $CHCl_3$-d_1) δ 8.12 (d, J = 2.5 Hz, 1H), 7.33 (s, 1H), 7.28 (d, J = 8.1 Hz, 1H), 7.09 (s, 1H), 6.46 (d, J = 2.4 Hz, 1H), 6.42 (dd, J = 8.2, 2.4 Hz, 1H), 5.29 (s, 1H), 4.56 (d, J = 5.8 Hz, 2H), 3.84 (s, 3H), 3.79 (s, 3H), 3.75 (s, 2H), 1.94 (m, 1H), 1.74 (m, 1H), 1.38 (s, 3H), 1.50 – 1.20 (m, 4H), 0.91 (t, J = 7.1 Hz, 3H). LC/MS (*m*/*z*) 460.29 [M+1].

(*R*)-2-((2-amino-7-chloropyrido[3,2-*d*]pyrimidin-4-yl)amino)-2-methylhexan-1-ol ((*R*)-29). Compound **28** (11 mg, 0.02 mmol) was treated with TFA (3 mL) and the mixture stirred for 3.5 h. The reaction mixture was concentrated under redcued pressure and co-evaporated with MeOH (3 x 20 mL). The residue was suspended in MeOH, filtered, and the

eluant stirred a further 16 h. The mixture was concentrated under reduced pressure to provide (*R*)-**29** (10.6 mg, 100%) as a TFA salt. ^{1}H NMR (400 MHz, MeOH-d_4) δ 8.59 (d, *J* = 2.1 Hz, 1H), 8.25 (s, 1H), 7.91 (d, *J* = 2.1 Hz, 1H), 3.97 (d, *J* = 11.3 Hz, 1H), 3.71 (d, *J* = 11.3 Hz, 1H), 2.15 – 2.04 (m, 1H), 1.97 – 1.87 (m, 1H), 1.54 (s, 3H), 1.37 – 1.33 (m, 4H), 0.92 (t, *J* = 7.0 Hz, 3H). LC/MS (*m*/*z*) 310.12 [M+1].

(*R*)-2-((2-amino-7-methylpyrido[3,2-*d*]pyrimidin-4-yl)amino)-2-methylhexan-1-ol ((*R*)-30). Compound **28** (26.1 mg, 0.057 mmol), methylboronic acid (14.6 mg, 0.22 mmol), tetrakis(triphenylphosphine)palladium(0) (16.9 mg, 0.12 mmol), potassium phosphate tribasic (27.4 mg, 0.13 mmol) in 1,4-dioxane (2.2 mL) and water (2.2 mL) was heated to 150°C in a microwave reactor for 30 min. The reaction was diluted with water (20 mL), extracted with EtOAc (3 x 20 mL) and the combined organics washed with water (50 mL), brine (50 mL), dried over Na_2SO_4, filtered, and concentrated under reduced pressure. The residue was subjected to silica gel chromatography eluting with 15-100% EtOAc-hexanes to provide (*R*)-2-((2-((2,4-dimethoxybenzyl)amino)-7-methylpyrido[3,2-*d*]pyrimidin-4-yl)amino)-2-methylhexan-1-ol (31.4 mg). H NMR (400 MHz, $CHCl_3$-d_1) δ 7.74 – 7.62 (m, 2H), 7.29 (d, *J* = 7.5 Hz, 1H), 6.47 (d, *J* = 2.4 Hz, 1H), 6.42 (dd, *J* = 8.3, 2.4 Hz, 1H), 4.57 (d, *J* = 5.8 Hz, 2H), 3.85 (s, 3H), 3.79 (s, 3H), 3.78 – 3.66 (m, 2H), 2.03 – 1.88 (m, 1H), 1.81 – 1.68 (m, 1H), 1.58 (s, 3H), 1.39 (s, 3H), 1.36 – 1.21 (m, 4H), 0.90 (t, *J* = 7.4 Hz, 3H). LC/MS (*m*/*z*) 440.31 [M+1].

(*R*)-2-((2-((2,4-dimethoxybenzyl)amino)-7-methylpyrido[3,2-*d*]pyrimidin-4-yl)amino)-2-methylhexan-1-ol (31.4 mg) was treated with TFA (3 mL) and the mixture stirred for 30 min. The reaction mixture was concentrated under reduced pressure and co-evaporated with MeOH (3 x 20 mL). The residue was subjected to reverse phase preparative HPLC (30%-70% CH_3CN in water with 0.1% TFA on a Synergi 4μ Polar-RP 80A Axia over a 20 min gradient) and the

product that was isolated was suspended in MeOH. The mixture was filtered and the eluant stirred for 16 h and then the mixture concentrated under reduced pressure to provide (*R*)-**30** (18.8 mg, 82% over two steps) as a TFA salt. ^{1}H NMR (400 MHz, MeOH-d_4) δ 8.47 (d, J = 1.7 Hz, 1H), 7.64 (dd, J = 1.9, 1.0 Hz, 1H), 3.97 (d, J = 11.2 Hz, 1H), 3.72 (d, J = 11.2 Hz, 1H), 2.51 (s, 3H), 2.15 – 2.04 (m, 1H), 1.96 – 1.85 (m, 1H), 1.54 (s, 3H), 1.42 – 1.31 (m, 4H), 0.92 (t, J = 6.9 Hz, 3H). LC/MS (*m*/*z*) 290.19 [M+1].

2-Amino-7-fluoropyrido[3,2-*d*]pyrimidin-4-ol (32). Methyl 3-amino-5-fluoropicolinate **31** (830 mg, 4.88 mmol), chloroformamidine hydrochloride (1.1 g, 9.8 mmol), dimethyl sulfone (4.6 g, 48.8 mmol) were charged into a sealed pressure tube and the mixture stirred and heated to 160°C for 1 h. The reaction mixture was allowed to cool, water (50 mL) was added and the solution stirred for 30 min. Solids were removed by filtration and the eluant was subjected to reverse phase preparative HPLC (2%-5% CH_3CN in water with 0.1% TFA on a Hydro-RP column over a 20 min gradient). Solvents were removed under reduced pressure and the residue azeotroped with MeOH (2 x) and CH_2Cl_2 (2 x) before sonication in Et_2O. Solids were removed by filtration and dried to provide **32** (210 mg, 24%). ^{1}H NMR (400 MHz, DMSO-d_6) δ 8.43 (d, J = 2.5 Hz, 1H), 7.48 (dd, J = 10.1, 2.5 Hz, 1H), 7.23 (s, 2H).^{19}F NMR (376 MHz, DMSO-d_6) δ -119.96. LC/MS (*m/z*) 181.0 [M+1].

High Throughput Cyropreserved PBMC Assay. Cryopreserved human PBMCs isolated from healthy donors were purchased from StemCell Technologies (Vancouver, Canada). Cell culture medium used was RPMI with L-Glutamine (Mediatech, Manassas, VA) supplemented with 10% fetal bovine serum (Hyclone, GE Healthcare, Logan, UT) and Penicillin-Streptomycin (Mediatech). Human TNFα, IL-12p40, and IFNα-2a 384-well capture plates, standards, buffers and processing reagents were obtained from MesoScale Discovery

Technologies (MSD; Rockville, MD). Cryopreserved human PBMCs (1x10e8 cells/ml) were thawed at 37°C and resuspended in 25 mL warm cell culture medium. The cells were pelleted at 200Xg (Beckman Avanti J-E) for 5 min and resuspended in 20 mL of fresh culture media. Cells were counted using a Cellometer (Nexcelcom Bioscience), adjusted to $2x10^6$ cells, and incubated for 2 hours in an incubator set at 37°C, 5% CO_2 to recover from cryopreservation. Compounds were serially diluted in DMSO at half-log steps to generate a 10-point dose range. Using a Bravo pipette equipped with a 384 well head (Agilent), 0.4 µL of compound was transferred to each well of a 384 well black, clear bottom plate (Greiner Bio-One, Germany) containing 30 µL of cell culture medium. Recovered PBMCs were then dispensed into the assay plate at 50 µL per well (100k cells/well) using the MicroFlow multichannel dispenser (Biotek). Final DMSO concentration was 0.5%. Positive controls used were 10 µM GS-651557 for the TNFα and IL-12p40 assays, and 10 µM GS-9620 for the IFNα-2a assay. DMSO was used as the negative control. The plates were incubated for 24 hours at 37°C. PBMCs in the assay plate were pelleted by centrifugation (Beckman Avanti J-E) at 200Xg for 5 min. Using a Biomek FX 384 well pipetting station (Beckman), conditioned culture medium (CCM) from the assay plate was transferred to MSD capture plates customized for each cytokine. For IFNα and IL-12p40 detection, 25 µL and 20 µL of CCM were added directly to each capture plate, respectively. For TNFα detection, CCM was diluted 1:10 in fresh culture medium, and 20 µL of diluted CCM was used. Serially diluted calibration standards for each cytokine were used to generate standard curves and establish assay linearity. The plates were sealed and incubated overnight at 4°C in a plate shaker (Titer Plate) set at 200 rpm. On the following day, antibodies specific for each cytokine were diluted 1:50 in MSD Diluent 100 antibody dilution buffer. Diluted antibodies were added to corresponding capture plates at 10 µL /well, and incubated at rt for 1-2 hours in the

shaker. The plates were washed with PBST buffer (3x, 60 µL/well) using a Biotek Multiflow plate washer. MSD Read Buffer diluted to 2X in deionized water and 35 µL/well was added via Biomek FX instrument. The plates were read immediately in a MSD6000 reader. Data were normalized to positive and negative controls in each assay plate. EC_{50} values represent compound concentrations at half-maximal effect based on normalized percent activation and calculated using 4-parameter logistic curve fit with Pipeline Pilot software (Accelrys, San Diego, CA).

HBV infected Primary Human Hepatocyte Assay has been previously described.[30]

HEK Innate Immune Receptor Reporter Assays, MT-4 Cell Viability Assay, Pharmacokinetic Methods, Structural modeling and Crystallography Methods. See supporting information. All in vivo studies were performed in accordance with local IACUC guidelines.

Associated Content

Supporting Information

The supporting information is available free of charge.

Pharmacokinetic Methods, Cell-Based Assays, Preparation of Amines, Molecular Modeling/Single Crystal X-ray Diffraction Methods, Appendix of final compound HPLC and NMR spectra, Molecular Formula Strings

Accession Codes

The PDB code for the TLR8 X-Ray structure of (*R*)-**7** is 6WML. Authors will release the atomic coordinates upon article publication.

Homology Models.

PDB 3W3M structure was used for the models of **6a**, (*R*)-**6d** and (*S*)-**6d**

Author Information

Corresponding Author

*E-mail: richard.mackman@gilead.com. Tel.: 650 522 5258.

ORCID: Richard L. Mackman: 0000-0001-8861-7205

Present Addresses

‡(J. Z.) Pharmacyclics, an Abbvie Company 999 East Arques Avenue, Sunnyvale, California 94085, United States

ǀ(J.C.) Horizon Therapeutics, Two Tower Place, 12th floor, South San Francisco, California 94080, United States

Acknowledgements

The authors would like to acknowledge the TLR8 protein used to determine the (*R*)-7 X-Ray structure complex was made available for purchase from Professor T. Shimizu, Graduate School of Pharmaceutical Sciences, University of Tokyo.

Abbreviations Used

BOP, (Benzotriazol-1-yloxy)tris(dimethylamino)phosphonium hexafluorophosphate; cccDNA, covalent closed circular DNA; CHB, chronic hepatitis B; CCM, cell culture media; CC_{50}, concentration for 50% cell viability loss; Dmb, 2,4-dimethoxybenzyl; HATU, (1-[Bis(dimethylamino)methylene]-1*H*-1,2,3-triazolo[4,5-b]pyridinium 3-oxide hexafluorophosphate; HBV, hepatitis B virus; HEK, human embryonic kidney cells; IACUC, International animal care and use committee; IFN, interferon; MEC, minimum effective concentration equivalent to a 3-fold increase in measurement over baseline; MSD, MesoScale discovery; PBMC, peripheral blood mononuclear cell; PBST, phosphate buffered saline with tween 20; PHH, primary human hepatocytes; TLR, Toll-like receptor; WHV, woodchuck hepatitis B virus.

Notes

The authors declare the following competing financial interests: The authors are current or former employees of Gilead Sciences and may own company stock.

References

1. O'Neill, L. A.; Golenbock, D.; Bowie, A. G. The History of Toll-like Receptors - Redefining Innate Immunity. *Nat. Rev*. **2013**;*13(6)*, 453-460.
2. Gorden, K. B.; Gorski, K. S.; Gibson, S. J.; Kedl, R. M.; Kieper, W. C.; Qiu, X., Tomai, M. A.; Alkan, S. S.; Vasilakos, J. P. Synthetic TLR Agonists Reveal Functional Differences Between Human TLR7 and TLR8. *J. Immunol*. **2005**, *174*, 1259-1268.
3. World Health Organigation (WHO). Hepatitis B. Fact sheet N°204. Available at: http://www.who.int/mediacentre/factsheets/fs204/en/ (accessed Nov 2, 2019).
4. Ott, J. J.; Stevens, G. A.; Groeger, J.; Wiersma, S. T. Global Epidemiology of Hepatitis B Virus Infection: New Estimates of Age-Specific HBsAg Seroprevalence and Endemicity. *Vaccine* **2012**, *30(12)*, 2212-2219.
5. Bertoletti, A.; Ferrari, C. Adaptive Immunity in HBV Infection. *J. Hepatol.* **2016**, *64(1)*, S71-S83.
6. Du, J.; Wu, Z.; Ren, S.; Wei, Y.; Gao, M.; Randolph, G. J.; Qu, C. TLR8 Agonists Stimulate Newly Recruited Monocyte-Derived Cells Into Potent APCs That Enhance HBsAg Immunogenicity. *Vaccine* **2010**, *28(38),* 6273-6281.
7. Schurich, A.; Pallett, L. J.; Lubowiecki, M.; Singh, H. D.; Gill, U. S.; Kennedy, P. T.; Nastouli, E.; Tanwar, S.; Rosenberg, W.; Maini, M. K. The Third Signal Cytokine IL-12 Rescues the Anti-Viral Function of Exhausted HBV-Specific CD8 T cells. *PLoS pathogens*, **2013**, 9 (3):e1003208.
8. Jo, J., Tan, A. T.; Ussher, J. E.; Sandalova, E.; Tang, X.-Z.; Tan-Garcia, A.; To, N.; Hong, M.; Chia, A.; Gill, U. S.; Kennedy, P. T.; Tan, K. C.; Lee, K. H.; Libero, G. D.; Gehring, A. J.; Willberg, C. B.; Klenerman, P.; Bertoletti, A. Toll-Like Receptor 8

Agonist and Bacteria Trigger Potent Activation of Innate Immune Cells in Human Liver. *PLoS pathogens*, **2014**;10 (6):e1004210.

9. Huang, L.-R., Wohlleber, D., Reisinger, F., Jenne, C. N., Cheng, R.-L., Abdullah, Z.; Schildberg, F. A.; Odenthal, M.; Dienes, H.-P.; Rooijen, N. V.; Schmitt, E.; Garbi, N.; Croft, M.; Kurts, C.; Kubes, P.; Protzer, U.; Heikenwalder, M.; Knolle, P. A. Intrahepatic Myeloid-Cell Aggregates Enable Local Proliferation of $CD8^+$ T Cells and Successful Immunotherapy Against Chronic Viral Liver Infection. *Nat. Immunol*. **2013**, *14(6)*, 574-583.
10. Biermer, M.; Puro, R.; Schneider, R. J. Tumor Necrosis Factor Alpha Inhibition of Hepatitis B Virus Replication Involves Disruption of Capsid Integrity Through Activation of NF-κB. *J. Virol*ogy **2003**, *77(7)*, 4033-4042.
11. Watashi, K.; Liang, G.; Iwamoto, M.; Marusawa, H.; Uchida, N.; Daito, T.; Kitamure, K.; Muramatsu, M.; Ohashi, H.; Kiyohara, T.; Suzuki, R.; Li, J.; Tong, S.; Tanaka, Y.; Murata, K.; Aizaki, H.; Wakita, T. Interleukin-1 and Tumor Necrosis Factor-α Trigger Restriction of Hepatitis B Virus Infection Via a Cytidine Deaminase Activation-Induced Cytidine Deaminase (AID). *J. Biol. Chem*. **2013**, *288(44)*, 31715-31727.
12. Isorce, N.; Testoni, B.; Locatelli, M.; Fresquet, J.; Rivoire, M.; Luangsay, S.; Zoulim, F.; Durantel, D. Antiviral Activity of Various Interferons and Pro-Inflammatory Cytokines in Non-Transformed Cultured Hepatocytes Infected with Hepatitis B Virus. *Antiviral Res*. **2016**, *130*, 36-45.
13. Roethle, P. A.; McFadden, R. M.; Yang, H.; Hrvatin, P.; Hui, H.; Graupe, M.; Gallagher, B.; Chao, J.; Hesselgesser, J.; Duatschek, P.; Zheng, J.; Lu, B.; Tumas, D. B.; Perry, J.; Halcomb, R. L. Identification and Optimization of Pteridinone Toll-like Receptor 7

(TLR7) Agonists for the Oral Treatment of Viral Hepatitis. *J. Med. Chem*. **2013**, *56(18)*, 7324-7333.

14. Tanji, H.; Ohto, U.; Shibata, T.; Miyake, K.; Shimizu, T. Structural Reorganization of the Toll-Like Receptor 8 Dimer Induced by Agonistic Ligands. *Science* **2013**, *339 (6126)*, 1426-1429.
15. Kokatla, H. P.; Yoo, E.; Salunke, D. B.; Sil, D.; Ng, C. F.; Balakrishna, R.; Malladi, S. S.; Fox, L. M.; David, S. A. Toll-like Receptor-8 Agonistic Activities in C2, C4, and C8 Modified Thiazolo[4,5-c]quinolines. *Org. Biomol. Chem*. **2013**, *11*, 1179-1198.
16. Miller, R. L.; Gerster, J. F.; Owens, M. L.; Slade H. B.; Tomai, M. A. Imiquimod Applied Topically: A Novel Immune Response Modifier and New Class of Drug. *Intl. J. Immunopharm*. **1999**, *21(1)*, 1-14.
17. Lu, H.; Dietsch, G. N.; Matthews, M.-A. H.; Yang, Y.; Ghanekar, S.; Inokuma, M.; Suni, M.; Maino, V. C.; Henderson, K. E.; Howbert, J. J.; Disis, M. L.; Hershberg, R. M. VTX-2337 Is a Novel TLR8 Agonist That Activates NK Cells and Augments ADCC. *Clin. Can. Res.* **2012**,*18(2)*, 499-509.
18. Beesu, M.; Caruso, G.; Salyer, A. C. D.; Khetani, K. K.; Sil, D.; Weerasinghe, M.; Tanji, H.; Ohto, U.; Shimizu, T.; David, S. A. Structure-Based Design of Human TLR8-Specific Agonists with Augmented Potency and Adjuvanticity. *J. Med. Chem*. **2015**, *58*, 7833-7849.
19. Beesu, M.; Salyer, A. C. D.; Trautman, K. L.; Hill, J. K.; David, S. A. Human Toll-like Receptor (TLR) 8-Specific Agonistic Activity in Substituted Pyrimidine-2,4-diamines. *J. Med. Chem*. **2016**, *59*, 8082-8093.

20. McGowan, D.; Herschke, F.; Pauwels, F.; Stoops, B.; Last, S.; Pieters, S.; Scholliers, A.; Thoné, T.; Schoubroeck, B. V.; Pooter, D. D.; Mostmans, W.; Khamlichi, M. D.; Embrechts, W.; Dhuyvetter, D.; Smyej, I.; Arnoult, E.; Demin, S.; Borghys, H.; Fanning, G.; Vlach, J.; Raboisson, P. Novel Pyrimidine Toll-Like Receptor 7 and 8 Dual Agonists to Treat Hepatitis B Virus. *J. Med. Chem*. **2016**, *59*, 7936-7949.

21. Bondy, S.; Chou, C.-H.; Watkins, W. J.; Chong, L. S.; Zhang, J. R.; Mishra, R. Pyrido(3,2-*d*)pyrimidines Useful For Treating Viral Infections. Patent WO2008/077651 A1, 2008.

22. Daffis, S.; Chamberlain, J.; Zheng, J.; Santos, R.; Rowe, W.; Mish, M. R.; Ramakrishnan, D.; Yon, C; Suresh, M; Menne, S.; Cote, P.; Delaney IV, W. E.; Fletcher, S. P.; Mackman, R. L. Sustained Efficacy and Seroconversion With the Selective Toll-Like Receptor 8 Agonist GS-9688 in the Woodchuck Model of Chronic Hepatitis B. *Intl. Liver Congress.* **2017**, April 19-23, Amsterdam, The Netherlands; Poster SAT-165.

23. Zhang, Z.; Ohto, U.; Shibata, T.; Taoka, M.; Yamauchi, Y.; Sato, R.; Shukla, N. M.; David, S. A.; Isobe, T.; Miyake, K.; Shimizu, T. Structural Analyses of Toll-like Receptor 7 Reveal Detailed RNA Sequence Specificity and Recognition Mechanism of Agonistic Ligands. *Cell Rep.* **2018**, *25*, 3371-3381.

24. Embrechts, W.; Herschke, F.; Pauwels, F.; Stoops, B.; Last, S.; Pieters, S.; Pande, V.; Pille, G.; Amssoms, K.; Smyej, I.; Dhuyvetter, D.; Scholliers, A.; Mostmans, W.; Dijck, K. V.; Schoubroeck, B. V.; Thone, T.; Pooter, D. D.; Fanning, G.; Jonckers, T. H. M.; Horton, H.; Raboisson, P.; McGowan, D. 2,4-Diaminoquinazolines as Dual Toll-like Receptor (TLR) 7/8 Modulators for the Treatment of Hepatitis B Virus. *J. Med. Chem*. **2018**, *61*, 6236-6246.

25. pKa Calculator: https://www.acdlabs.com/products/percepta/predictors/pka/index.php; ACD Labs.

26. Harwood, L. M.; Vines, K. J.; Drew, M. G. B. Synthesis of Homochiral α-Substituted Alanine Derivatives by Daistereocontrolled Alkylation of (5R)-5-Phenyl-3-methyl-3,4-dehydromorpholinones. *Synlett* **1996**, *11*, 1051-1053.

27. Menne, S.; Tumas, D. B.; Liu, K. H.; Thampi, L.; AlDeghaither, D.; Baldwin, B. H.; Bellezza, C. A.; Cote, P. J.; Zheng, J.; Halcomb, R.; Fosdick, A.; Fletcher, S. P.; Daffis, S.; Li, L.; Yue, P.; Wolfgang, G. H. I.; Tennant, B. C. Sustained Efficacy and Serconversion with the Toll-like Receptor 7 Agonist GS-9620 in the Woodchuck Model of Chronic Hepatitis B. *J. Hepatol.* **2015**, *62(6)*, 1237-1245.

28. Daffis, S.; Balsitis, S.; Chamberlain, J.; Zheng, J.; Santos, R.; Rowe, W.; Ramakrishnan, D.; Pattabiraman, D.; Spurlock, S.; Chu, R.; Kang, D.; Mish, M.; Ramirez, R.; Li, L.; Li, B.; Ma, S.; Hung, M.; Voitenleitner, C.; Yon, C.; Suresh, M.; Menne, S.; Cote, P.; Delaney IV, W. E.; Mackman R.; Fletcher, S. P. Toll-Like Receptor 8 Agonist GS-9688 Induces Sustained Efficacy in the Woodchuck Model of Chronic Hepatitis B. *Hepatol.* in press.

29. Tikad, A.; Akssira, M.; Massip, S.; Léger, J.-M.; Jarry, C.; Guillaumet, G.; Routier, S. Regiocontroled S_NAr and Palladium Cross-Coupling Reactions of 2,4,7-Trichloropyrido[3,2-*d*]pyrimidine. *Eur. J. Org. Chem*. **2012**, 4523-4532.

30. Niu, C.; Li, L.; Daffis, S.; Lucifora, J.; Bonnin, M.; Maadadi, S.; Salas, E.; Chu, R.; Ramos, H.; Livingston, C. M.; Beran, R. K.; Garg, A. V.; Balsitis, S.; Durantel, D.; Zoulim, F.; Delaney, W. E. IV; Fletcher S. P. Toll-like Receptor 7 Agonist GS-9620

Induces Prolonged Inhibition of HBV Via a Type I Interferon-Dependent Mechanism. *J. Hepatol.* **2018**, *68(5)*, 922-931.